Inorg. Chem. **2007**, *46*, 9351–9363

Comparisons of Phosphorus Ligation Properties in $P(CH_2NR)_3P$

Natesan Thirupathi,[†] Phillip M. Stricklen, Xiaodong Liu, Reed Oshel, Ilia Guzei, Arkady Ellern, and John G. Verkade*

Department of Chemistry, Iowa State University, Ames, Iowa 50011-3111

Received February 15, 2007

Bicyclic $P(CH_2NMe)_3P$ was synthesized, and its reactions with MnO_2, elemental sulfur, *p*-toluenesulfonyl azide, BH_3·THF, and $W(CO)_5(THF)$ were shown to furnish a variety of products in which the PC_3 and/or the PN_3 phosphorus are oxidized/coordinated. In contrast, reactions of the previously known $P(CH_2NPh)_3P$ with Mo(0) and Ru(II) precursors were shown to afford products in which only the PC_3 phosphorus is coordinated. The contrast in reactivity of $P(CH_2NR)_3P$ (R = Me, Ph) with the aforementioned reagents is discussed in terms of steric and electronic factors. The new compounds are characterized by analytical and spectroscopic (IR, ^1H, ^{31}P, and ^{13}C NMR) methods. The results of crystal and molecular structure X-ray analyses of the previously known compounds $P(CH_2O)_3P$ and $P(CH_2NPh)_3P$ and 6 of the 14 new compounds obtained in this investigation are presented. Salient features of these structures and the analysis of the Tolman cone angles calculated from their structural parameters are discussed in terms of the effects of constraint in the bicyclic moieties. Evidence is presented for greater M–P σ bonding effects on coordination of the PC_3 phosphorus of $P(CH_2NR)_3P$ (R = Me, Ph) than are present in PMe_3 analogues of group 6B metal carbonyls. From $^1J_{BP}$ data on the BH_3 adducts of $P(CH_2NMe)_3P$, it is suggested that the free bases $MeC(CH_2NMe)_3P < P(CH_2NMe)_3P < (Me_2N)_3P < P(MeNCH_2CH_2)_3N$ increase in Lewis basicity at the PN_3 phosphorus in the order shown. Substantial differences in ^{31}P chemical shifts in the bicyclic compounds discussed herein relative to their acyclic analogues do not seem to be associated with the relatively small bond angle changes that occur around either the PN_3 or the PC_3 trivalent phosphorus atoms.

Introduction

Bicyclic molecules of the types shown below possessing two bridgehead phosphorus atoms are interesting because of their high symmetry and their potential for donating an electron pair to one or two acceptors.

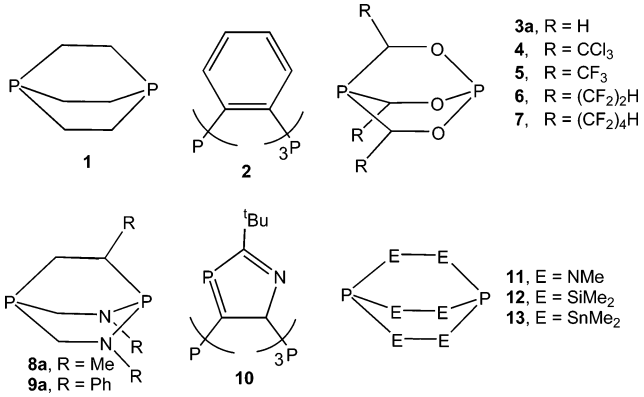

Although the synthesis of **1** was reported along with a few of its derivatives over 45 years ago,[1] no further results with **1** have been described. Bicyclic **2**[2] as well as its perfluoro[3] and perchloro[4] aromatic analogues have been reported, and the dioxide[5a] and protonated form[5b] of perhydro **2** are also known. In 1965 our group and others reported various syntheses of **3a**.[6] Although phosphines are usually considered to be more Lewis basic than phosphites, the PO_3 phosphorus

* To whom correspondence should be addressed. E-mail: jverkade@iastate.edu.

[†] Current address: Department of Chemistry, University of Delhi, Delhi 110 007, India.

(1) Hinton, R. C.; Mann, F. G. *J. Chem. Soc*. **1959**, 2885−2943.
(2) (a) Weinberg, K. G. *J. Org. Chem.* **1975**, *40*, 3586−3589. (b) Weinberg, K. G.; Whipple, E. B. *J. Am. Chem. Soc.* **1971**, *93*, 1801−1802.
(3) Al-Jabar, N. A. A.; Massey, A. G. *J. Organomet. Chem.* **1985**, *287*, 57−64.
(4) (a) Massey, A. G. *Adv. Inorg. Chem.* **1989**, *33*, 1−38. (b) Al-Jabar, N. A. A.; Jones, J. B.; Brown, D. S.; Colligan, A. H.; Massey, A. G.; Miller, J. M.; Nye, J. W. *Appl. Organomet. Chem.* **1989**, *3*, 459−468.
(5) (a) Schomburg, D.; Sheldrick, W. S. *Acta Crystallogr., Sect. B: Struct. Crystallogr. Cryst. Chem.* **1975**, *B31*, 2427−2431. (b) Vande Griend, L. J.; Verkade, J. G.; Jongsma, C.; Bickelhaupt, F. *Phosphorus Relat. Elem.* **1976**, *6*, 131−133.
(6) (a) Coskran, K. J.; Verkade, J. G. *Inorg. Chem.* **1965**, *4*, 1655−1657. (b) Rathke, J. W.; Guyer, J. W.; Verkade, J. G. *J. Org. Chem.* **1970**, *35*, 2310−2313. (c) Kisanga, P.; Verkade, J. G. *Heteroat. Chem.* **2001**, *12*, 114−117. (d) Kozlov, E. S; Tovstenko, V. I. *Zh. Obshch. Khim.* **1980**, *50*, 1499−1501. (e) Volcko, E. J.; Verkade, J. G. *Phosphorus Sulfur* **1984**, *21*, 111−118.

10.1021/ic0703070 CCC: $37.00
Published on Web 09/25/2007

of **3a** was shown to react preferentially with chalcogens and transition metals, and evidence consistent with better π-acceptor properties of the PO_3 phosphorus was presented.[6a,7−10] A variety of nonmetal derivatives (**3b**−**k**) and transition metal complexes (**3l**−**x**) of **3a** have appeared in the literature.[6a,7−11] R groups other than H in **3a** (i.e., **4**−**7**), halo derivatives $P(RCHO)_3PX_2$ of **4**−**6**, oxo derivatives $P[C(R)HO]_3P{=}O$ and $OP[C(CCl_3)HO]_3P$ of **4**−**6**, and $P[C(CCl_3)HO]_3P{=}NTs$ have also been synthesized.[12−16]

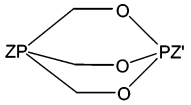

	Z	Z'		Z	Z'
3b	O	lp	**3j**	O	S
3c	lp	O	**3k**	lp	$Me^+BF_4^-$
3d	O	O	**3l-n**	lp	$M(CO)_5$ [M = Cr (**3l**), Mo (**3m**), W(**3n**)]
3e	S	lp	**3o-q**	$M(CO)_5$	$M(CO)_5$[M = Cr (**3o**), Mo (**3p**), W(**3q**)]
3f	lp	S	**3r**	$Fe(CO)_4$	lp
3g	S	S	**3s**	lp	$Fe(CO)_4$
3h	lp	BH_3	**3t**	$Fe(CO)_4$	$Fe(CO)_4$
3i	BH_3	BH_3			

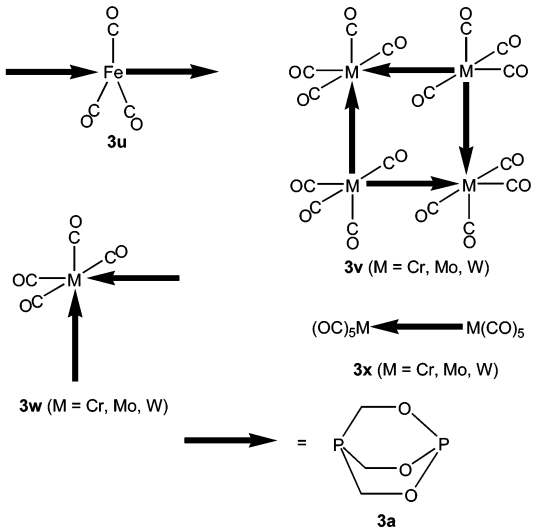

Compounds **8a**[17] and **9a**[17] have been reported by us, as has been an improved route to **9a**.[6c] A multistep synthesis of **10** has been described,[18] and bicyclic diphosphines bearing N−N (**11**[19]), Si−Si (**12**[20]), or Sn−Sn (**13**[21]) linkages are known. Derivatives of **11** in which both phosphorus atoms are bonded to BH_3,[19a,b] $W(CO)_5$,[19c] NPh,[19c,d] S,[19a] or O[19e] are also known.

In an effort (i) to delineate the factors that dictate the reactivity of the PC_3 versus PN_3 phosphorus (or PO_3 phosphorus in case of **3a**) and (ii) to utilize **8a** and **9a** as ligands for constructing bis-ligated dinuclear and macrocyclic tetranuclear metal complexes as we reported with **3a**[6−11] (e.g., **3o**−**q**, **3t**,**v**,**x**) we synthesized (a) bicyclic **8a**, six of its nonmetal derivatives **(8b**−**g),** and two of its transition metal complexes **(8h**,**i)**, (b) transition metal complexes of **9a** (i.e., **9b** and **9d**−**f**), and (c) a molybdenum tetracarbonyl complex of **8b (**i.e., **8l)**. Spectroscopic evidence for **9c** as an intermediate formed during the synthesis of **9d** is put forth. The results of crystal and molecular structure X-ray analyses of the previously known compounds **3a** and **9a** and the new compounds **8b**,**f**,**i** and **9d**,**e**,**f** are presented, and Tolman cone angles ranging from 106 to 220° were calculated for **3a**, **8b**,**f**,**i**, and **9a**,**d**,**e**,**f** from their X-ray parameters.

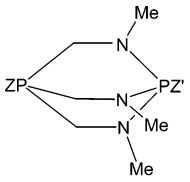

	Z	Z'		Z	Z'
8b	O	lp	**8g**	9-BBN	lp
8c	S	S	**8h**	$W(CO)_5$	lp
8d	NTs	NTs	**8i**	$W(CO)_5$	$W(CO)_5$
8e	lp	BH_3	**8j**	O	N_3Ts
8f	BH_3	BH_3	**8k**	O	NTs

cis/*trans*-$Mo(CO)_4[P(NMeCH_2)_3P{=}O]_2$ (**8l**)

Experimental Section

General Methods. All reactions were carried out under argon. Solvents were purified by standard procedures prior to use,[22] and the following compounds were prepared by published methods: (η^5-C_5Me_5)RuCl(COD),[23] **3a**,[6a] and **9a**,[6c] as well as $P(CH_2NHPh)_3$[24] that was used to prepare **9a**. $[P(CH_2OH)_4]_2SO_4$ (a generous donation

(7) Allison, D. A.; Verkade, J. G. *Phosphorus* **1973**, *2*, 257−264.
(8) Clardy, J. C.; Dow, D. C.; Verkade, J. G. *Phosphorus* **1975**, *5*, 85−89.
(9) Stricklen, P. M.; Volcko, E. J.; Verkade, J. G. *J. Am. Chem. Soc.* **1983**, *105*, 2494−2495.
(10) Bertrand, R. D.; Allison, D. A.; Verkade, J. G. *J. Am. Chem. Soc.* **1970**, *92*, 71−77.
(11) Allison, D. A.; Clardy, J. C.; Verkade, J. G. *Inorg. Chem.* **1972**, *11*, 2804−2809.
(12) Shermolovich, Y. G.; Danchenko, E. A.; Solov'ev, A. V.; Markovskii, L. N. *Zh. Obshch. Khim.* **1985**, *55*, 2218−2226.
(13) Kozlov, E. S.; Solov'ev, A. V.; Markovskii, L. N. *Zh. Obshch. Khim.* **1978**, *48*, 2437−2442.
(14) Chernega, A. N.; Tumanskii, B. L.; Antipin, M. Y.; Solodovnikov, S. P.; Bubnov, N. N.; Prokof'ev, A. I.; Struchkov, Y. T.; Kozlov, E. S.; Boldeskul, I. E.; Kabachnik, M. I. *Zh. Obshch. Khim.* **1986**, *56*, 546−552.
(15) Shermolovich, Y. G.; Danchenko, E. A.; Solov'ev, A. V.; Trachevskii, V. V.; Markovskii, L. N. *Zh. Obshch. Khim.* **1986**, *56*, 560−567.
(16) Markovskii, L. N.; Solov'ev, A. V.; Pirozhenko, V. V.; Shermolovich, Y. G. *Zh. Obshch. Khim.* **1981**, *51*, 1950−1956.
(17) Stricklen, P. M. Ph.D. Dissertation, Iowa State University, Ames, IA, 1970.
(18) Keller, H.; Regitz, M. *Tetrahedron Lett.* **1988**, *29*, 925−928.
(19) (a) Goetze, R.; Noth, H.; Payne, D. S. *Chem. Ber.* **1972**, *105*, 2637−2653. (b) Kroshefsky, R. D.; Verkade, J. G. *Phosphorus Sulfur* **1979**, *6*, 397−405. (c) Kroshefsky, R. D.; Verkade, J. G.; Pipal, J. R. *Phosphorus Sulfur* **1979**, *6*, 377−389. (d) Bermann, M.; Van Wazer, J. R. *Inorg. Chem.* **1974**, *13*, 737−738. (e) Gilje, J. W.; Seff, K. *Inorg. Chem.* **1972**, *11*, 1643−1646.
(20) (a) Winkler, U.; Schieck, M.; Pritzkow, H.; Driess, M.; Hyla-Kryspin, I.; Lange, H.; Gleiter, R. *J. Chem. Eur.* **1997**, *3*, 874−880. (b) Kolleger, G. M.; Katzenbeisser, U.; Hassler, K.; Kruger, C.; Brauer, D.; Gielen. R. *J. Organomet. Chem.* **1997**, *543*, 103−110.
(21) Draeger, M.; Mathiasch, B. *Angew. Chem.* **1981**, *93*, 1079−1080.
(22) Amerego, W. L. F.; Perrin, D. D. *Purification of Laboratory Chemicals*, 4th ed.; Butterworth and Heinemann: Oxford, U.K., 1996.

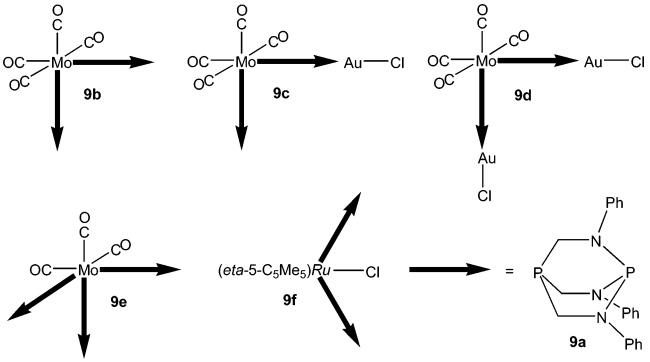

from Albright & Wilson, Americas), BH_3·THF, 9-BBN, and Mo(CO)$_4$(NBD) (Aldrich), and W(CO)$_6$ and Mo(CO)$_3$(CHT) (Strem) were used as received. W(CO)$_5$(THF) was prepared in situ by irradiating a quartz Schlenk flask (20 cm length × 3.0 cm diameter) containing an appropriate amount of W(CO)$_6$ in THF for 12 h with a 450 W 4.3 in. water-cooled UV immersion lamp (Ace Glass Inc.). Details of the melting points, elemental analyses, electrospray ionization (ESI) mass spectral analyses, and NMR (^{1}H, ^{13}C, and ^{31}P) and IR spectroscopies were previously described.[25] ^{1}H-decoupled ^{11}B NMR spectra were recorded on a Bruker WM-200 NMR spectrometer using BF_3·Et_2O as the external standard. Single crystals of **3a** were obtained by slow sublimation (82 °C/400 mTorr). Single crystals of **9a** were obtained by cooling an EtOAc solution of **9a** to −30 °C. Anal. Calcd for $C_{21}H_{21}N_3P_2$: C, 66.84; 5.60; N, 11.13. Found: C, 65.85/65.84; H, 5.78/5.81; N, 11.12/11.06.

P(CH$_2$NMe)$_3$P (8a). A 75% aqueous solution of [P(CH$_2$OH)$_4$]$_2$SO$_4$ (167.7 g, 410.2 mmol) was dissolved in distilled water (205 mL), and the resulting solution was purged with nitrogen for 12 h while being stirred. Under continued stirring at 0 °C, a 40% aqueous solution of methylamine (143.0 g, 1.841 mol) was slowly added. The temperature was slowly raised to 25 °C, and stirring was continued for an additional 12 h. The aminophosphine P(CH$_2$NMeH)$_3$ and aminophosphine oligomers were extracted with dichloromethane (5 × 50 mL), and the extracts were stored over Na_2SO_4. Dichloromethane was removed under reduced pressure to give a mixture that contained a colorless free-flowing oil and a semisolid (47.02 g). The free-flowing oil, which was decanted from the semisolid, was used for subsequent reactions. Attempts to obtain pure P(CH$_2$NMeH)$_3$ by vacuum distillation were unsuccessful. ^{1}H-decoupled ^{31}P NMR ($CDCl_3$) for the mixture of P(CH$_2$NMeH)$_3$ and aminophosphine oligomers: δ −59.9 (br). Reliable ^{1}H and ^{13}C NMR spectral assignments could not be made for P(CH$_2$NMeH)$_3$.

A 47.02 g sample of P(CH$_2$NMeH)$_3$/aminophosphine oligomers was charged to a 500 mL flask under dry nitrogen. The flask was heated to 95 °C under stirring, and then P(NMe$_2$)$_3$ (48.77 g, 300.0 mmol) was slowly added over a period of 1 h. When the addition was complete, the temperature was raised to 135 °C with stirring for 24 h after which the mixture was allowed to cool to room temperature. The free flowing orange liquid was transferred to another flask and vacuum distilled (42 °C/12 mTorr). The distillate (52.16 g) was shown to contain approximately 40% of **8a** as estimated by ^{1}H NMR spectroscopy. The remaining material (presumably aminophosphine oligomers) showed broad ^{31}P NMR resonances at −33.26, −39.98, −56.36, and −58.52 ppm. An estimate of the amount of **8a** in the reaction mixture was made as follows. The aminophosphine oligomers were selectively removed by transferring 100 mg of the distilled material into a 5 mm NMR tube that contained ca. 1.0 mL of cyclohexane. A 3.0% aqueous H_2O_2 solution was added dropwise to this solution while the reaction was monitored by ^{31}P NMR spectroscopy. The aminophosphine oligomers after oxidation were found in the water layer, leaving **8a** in the cyclohexane. When the oligomers were completely oxidized, H_2O_2 addition was stopped because **8a** reacted with H_2O_2 to destroy the cage.

From the above ^{31}P NMR experiment, the amount of H_2O_2 required to oxidize the aminophosphine oligomers for the rest of the distilled material was calculated, and then the scaled up oxidation experiment was carried out at 0 °C in 500 mL of cyclohexane. The oxidized impurities were extracted into the water layer, the cyclohexane layer was dried over Na_2SO_4, and the solvent was removed under reduced pressure leaving **8a** as a colorless liquid in 25% overall yield. ^{31}P{^{1}H} NMR (C_6D_6): δ −53.1 (d, PC_3), 82.3 (br d, PN_3), $^3J_{PP}$ 26.6 Hz. ^{1}H NMR (C_6D_6): δ 2.54 (d, $^3J_{PH}$ 16.76 Hz, NCH_3, 9H), 2.78 (dd, $^2J_{PH}$ 7.16 Hz; $^3J_{PH}$ 3.40 Hz, NCH_2, 6H). ^{13}C{^{1}H} NMR (C_6D_6): δ 43.0 (d, $^2J_{PC}$ 34.50 Hz, NCH_3, 3C), 44.9 (d, $^1J_{PC}$ 12.13 Hz, NCH_2, 3C). ESI-MS (*m*/*z*): 192 (M + H)$^+$, 177 (M − Me)$^+$. Anal. Calcd for $C_6H_{15}N_3P_2$: C, 37.70; H 7.91; N, 21.98. Found: C, 37.67/37.70; H, 7.94/8.01; N, 21.79/21.93.

O=P(CH$_2$NMe)$_3$P (8b). To a toluene (25 mL) solution of **8a** (1.19 g, 6.22 mmol) was added 85% activated MnO_2 (3.28 g, 37.7 mmol), and the mixture was refluxed for 2 h. After being cooled to room temperature, the solution was filtered and toluene was removed under reduced pressure giving **8b** as a hygroscopic white solid. Yield: 53%. Crystals were grown by vapor diffusion of pentane into a benzene solution of **8b**. Mp: 155 °C. IR (Nujol, cm^{-1}): $\nu_{P=O}$ 1319 (m). ^{31}P{^{1}H} NMR ($CDCl_3$): δ 35.6 (d, PC_3), 81.5 (d, PN_3), $^3J_{PP}$ 13.7 Hz. ^{1}H NMR ($CDCl_3$): δ 2.67 (dd, $^3J_{PH}$ 16.4 Hz; $^4J_{PH}$ 2.4 Hz, NCH_3, 9H), 3.18 (dd, $^2J_{PH}$ 12.80 Hz; $^3J_{PH}$ 2.92 Hz, NCH_2, 6H). ^{13}C{^{1}H} NMR ($CDCl_3$): δ 42.2 (dd, $^2J_{PC}$ 30.3 Hz, $^3J_{PC}$ 8.34 Hz, NCH_3, 3C), 47.7 (dd, $^1J_{PC}$ 68.99 Hz; $^2J_{PC}$ 4.17 Hz, NCH_2, 3C). Anal. Calcd for $C_6H_{15}N_3P_2O$: C, 34.78; H 7.30; N, 20.28. Found: C, 34.24/34.22; H, 7.30/7.46; N, 19.75/19.52.

S=P(CH$_2$NMe)$_3$P=S (8c). To a benzene (80 mL) solution of **8a** (4.00 g, 20.9 mmol) was added elemental sulfur (1.70 g, 53.0 mmol) in small portions over 30 min. The solution was refluxed for 2 h, cooled, and filtered. Benzene was removed from the filtrate to give a white solid to which cyclohexane (50 mL) was added. The mixture was refluxed for 1 h and filtered hot to remove cyclohexane-soluble impurities. After drying the cyclohexane-insoluble material in vacuo, acetone (100 mL) was added and the mixture was heated to reflux for 1 h and filtered hot to give a white solid consisting of 1.20 g of pure **8c**. Acetone was removed from the filtrate in vacuo to give a solid that was dissolved in chloroform and filtered; the filtrate was concentrated to give a green paste from which impurities were removed by washing with acetone, providing an additional 700 mg of **8c**. Total yield: 30%. Mp: 228 °C. ^{31}P-{^{1}H} NMR ($CDCl_3$): δ 34.6 (d, PC_3), 62.5 (d, PN_3), $^3J_{PP}$ 107.8 Hz. ^{1}H NMR ($CDCl_3$): δ 2.90 (dd, $^3J_{PH}$ 12.12 Hz; $^4J_{PH}$ 2.74 Hz, NCH_3, 9H), 3.64 (apparent t, $^2J_{PH}$ $^3J_{PH}$ 7.42 Hz, NCH_2, 6H). ^{13}C-{^{1}H} NMR ($CDCl_3$): δ 40.2 (d, $^2J_{PC}$ 3.37 Hz, NCH_3, 3C), 54.2 (d, $^1J_{PC}$ 47.17 Hz, NCH_2, 3C). Anal. Calcd for $C_6H_{15}N_3P_2S_2$: C, 28.23; H 5.92; N, 16.46; S, 25.12. Found: C, 28.30/28.39; H, 5.55/5.76; N, 16.49/16.45; S, 25.06/24.96.

TsN=P(CH$_2$NMe)$_3$P=NTs (8d). To a stirred acetone (50 mL) solution of **8a** (2.06 g, 10.8 mmol) was slowly added tosyl azide (4.25 g, 21.6 mmol) whereupon immediate gas evolution was

(23) Fagan, P. J.; Mahoney, W. S.; Calabrese, J. C.; Williams, I. D. *Organometallics* **1990**, *9*, 1843−1852.
(24) Frank, A. R.; Drake, G. L., Jr. *J. Org. Chem.* **1972**, *37*, 2752−2755.
(25) Thirupathi, N.; Liu, X.; Verkade, J. G. *Inorg. Chem.* **2003**, *42*, 389−397.

observed. The mixture was stirred for an additional 15 h; then acetone was removed under reduced pressure to give a solid to which diethyl ether (15 mL) was added, and the mixture was stirred for 30 min. The ether-insoluble material was collected by filtration and dried under reduced pressure to give **8d** in quantitative yield. Purified **8d** for elemental analysis was obtained by crystallization via vapor diffusion of pentane into a $CHCl_3$ solution. Mp: 230 °C. $^{31}P\{^1H\}$ NMR ($CDCl_3$): δ 1.7 (d, PC_3), 20.0 (d, PN_3), $^3J_{PP}$ 115.1 Hz. ^1H NMR ($CDCl_3$): δ 2.39, 2.41 (each s, $C_6H_4CH_3$-4, 6H), 2.91 (dd, $^3J_{PH}$ 11.08 Hz, $^4J_{PH}$ 2.76 Hz, NCH_3, 9H), 3.79 (apparent t, $^2J_{PH}$, $^3J_{PH}$ 8.68 Hz, NCH_2, 6H), 7.25, 7.75 (m, C_6H_4, 8H). $^{13}C\{^1H\}$ NMR ($CDCl_3$): δ 21.6, 21.7 (each s, $C_6H_4CH_3$-4, 2C), 39.5 (d, $^2J_{PC}$ 1.14 Hz, NCH_3, 3C), 48.3 (dd, $^1J_{PC}$ 60.27 Hz, $^2J_{PC}$ 2.27 Hz, NCH_2, 3C), 125.8, 129.5, 142.0 (m, C_6H_4, 12C). Anal. Calcd for $C_{20}H_{29}N_5O_4P_2S_2$: C, 45.36; H, 5.52; N, 13.22; S, 12.11. Found: C, 45.08/45.08; H, 5.72/5.72; N, 13.19/13.17; S, 12.06/11.96.

$P(CH_2NMe)_3P{\cdot}BH_3$ (8e). To a stirred solution of **8a** (2.06 g, 10.8 mmol) in THF (50 mL) was slowly added a 1.0 M THF solution of $BH_3{\cdot}$THF (11.0 mmol, 11.0 mL). The mixture was stirred for 15 h, and then THF was removed under reduced pressure to give a gum to which was added pentane (15 mL) followed by stirring for 30 min. After filtration, the pentane-insoluble material was dried under reduced pressure to give a solid that was dissolved in CH_2Cl_2 (10 mL) and filtered. Hexanes were added to the filtrate to obtain **8e** as a white precipitate in 69% yield (1.57 g). Mp: 114 °C. $^{31}P\{^1H\}$ NMR ($CDCl_3$): δ −56.4 (d, PC_3), 84.3 (four-line pattern, $^1J_{PB}$ 88.5 Hz, PN_3), $^3J_{PP}$ 8.6 Hz. $^{11}B\{^1H\}$ NMR ($CDCl_3$): δ −43.5 (d, PN_3, $^1J_{PB}$ 87.2 Hz BH_3, 1 B). ^1H NMR ($CDCl_3$): δ 0.47 (quartet of doublets, $^1J_{BH}$ 96.24 Hz; $^2J_{PH}$ 17.16 Hz, BH_3, 3H), 2.69 (d, $^3J_{PH}$ 13.64 Hz, NCH_3, 9H), 3.24 (dd, $^2J_{PH}$ 6.40 Hz; $^3J_{PH}$ 5.68 Hz, NCH_2, 6H). $^{13}C\{^1H\}$ NMR ($CDCl_3$): δ 40.3 (d, $^2J_{PC}$ 6.82 Hz, NCH_3, 3C), 46.5 (dd, $^1J_{PC}$ 18.57 Hz, $^2J_{PC}$ 4.93 Hz, NCH_2, 3C). Anal. Calcd for $C_6H_{18}N_3P_2B$: C, 35.15; H 8.85; N, 20.50. Found: C, 35.03/34.95; H, 8.92/8.87; N, 19.77/19.85.

$H_3B{\cdot}P(CH_2NMe)_3P{\cdot}BH_3$ (8f). To a stirred solution of **8a** (0.635 g, 3.32 mmol) in THF (40 mL) was slowly added a 1.0 M THF solution of $BH_3{\cdot}$THF (7.0 mmol, 7.0 mL), and stirring was continued for 15 h. THF was removed under reduced pressure to give a solid to which Et_2O (15 mL) was added. The mixture was stirred for 30 min and filtered, and the ether-insoluble material was dried under reduced pressure to give a solid. The solid was dissolved in CH_2Cl_2 (10 mL) and filtered, and the filtrate was concentrated to give **8f** as a white solid in 40% yield (0.293 g). Crystals for X-ray analysis were grown by pentane vapor diffusion into a benzene solution of **8f**. Mp: 150 °C. $^{31}P\{^1H\}$ NMR ($CDCl_3$): δ 4.5 (br, PC_3), 87.3 (br m, PN_3). $^{11}B\{^1H\}$ NMR ($CDCl_3$): δ −42.9, −44.1 (each br, BH_3, 2B). ^1H NMR ($CDCl_3$): δ 0.47 (four-line pattern, $^1J_{BH}$ 96.0 Hz, BH_3, 6H), 2.75 (dd, $^3J_{PH}$ 13.28 Hz; $^4J_{PH}$ 1.20 Hz, NCH_3, 9H), 3.38 (apparent t, $^2J_{PH}$, $^3J_{PH}$ 4.92 Hz, NCH_2, 6H). $^{13}C\{^1H\}$ NMR ($CDCl_3$): δ 40.4 (dd, $^2J_{PC}$ 6.45 Hz, $^3J_{PC}$ 4.55 Hz, NCH_3, 3C), 46.1 (dd, $^1J_{PC}$ 28.81 Hz; $^2J_{PC}$ 5.68 Hz, NCH_2, 3C). Anal. Calcd for $C_6H_{21}N_3P_2B_2$: C, 32.93; H 9.67; N, 19.20. Found: C, 32.85/32.91; H, 9.65/9.78; N, 19.17/19.15.

Reaction of 8a with 9-BBN. A 0.5 M THF solution of 9-BBN (1.61 mL, 805 μmol) was slowly added to a 5 mm NMR tube containing **8a** (154 mg, 805 μmol). The reaction mixture was briefly shaken, and then the ^{31}P NMR spectrum was recorded after 15 min revealing the formation of a new species in addition to **8a**. The structure of the new species was assigned to **8g**. The intensity of the ^{31}P NMR signals corresponding to **8g** increased relative to that corresponding to **8a** over 24 h. The ^{31}P NMR spectrum recorded after ca. 4 days indicated the presence of **8a**,**g** and several unidentified species. Because of the equilibrium involving **8a**,**g**, the latter could not be isolated. ^{31}P NMR (THF) for **8g**: δ_P −8.1 (br, PC_3), 84.4 (d, $^3J_{PP}$ 9.77 Hz, PN_3).

$W(CO)_5[P(CH_2NMe)_3P]$ (8h). $W(CO)_5$(THF) was prepared in situ as mentioned earlier from $W(CO)_6$ (2.00 g, 5.68 mmol) and THF (200 mL). This solution was slowly added to a stirred solution of **8a** (1.50 g, 7.85 mmol) in THF (20 mL). The mixture was stirred for an additional 15 h after which THF and unreacted **8a** were removed by evaporation under reduced pressure to furnish a colorless solid which was dissolved in pentane and filtered, and the filtrate was concentrated under reduced pressure to give **8h** as a white powder in 48% yield [based on $W(CO)_6$]. A pure sample of **8h** was obtained by sublimation (120 °C/300 mtorr). Mp: 108−110 °C. IR (Nujol, cm^{-1}): ν_{CO} 2072 (s), 1943 (s, br), 1913 (s, sh). $^{31}P\{^1H\}$ NMR($CDCl_3$): δ −23.2 (d, $^1J_{WP}$ 118.0 Hz, PC_3),79.0 (d, PN_3), $^3J_{PP}$ 16.3 Hz. ^1H NMR ($CDCl_3$): δ 2.70 (dd, $^3J_{PH}$ 16.47 Hz, $^4J_{PH}$ 1.35 Hz, NCH_3, 9H), 3.24 (dd, $^2J_{PH}$ 3.06 Hz, $^3J_{PH}$ 1.59 Hz, NCH_2, 6H). $^{13}C\{^1H\}$ NMR ($CDCl_3$): δ 42.2 (dd, $^2J_{PC}$ 33.69 Hz, $^3J_{PC}$ 5.05 Hz, NCH_3, 3C), 50.0 (dd, $^1J_{PC}$ 26.95 Hz, $^2J_{PC}$ 3.37 Hz, NCH_2, 3C), 195.3 (d, $^2J_{PC}$ 6.74 Hz, $^1J_{WC}$ 62.33 Hz, *cis*-CO, 4C), 198.3 (d, $^2J_{PC}$ 21.90 Hz, *trans*-CO, 1C). Anal. Calcd for $C_{11}H_{15}N_3O_5P_2W$: C, 25.65; H 2.94; N, 8.16. Found: C, 25.38/25.33; H, 2.93/2.91; N, 8.08/8.03.

$W(CO)_5[P(CH_2NMe)_3P]W(CO)_5$ (8i). Freshly sublimed **8h** (1.18 g, 2.29 mmol) was dissolved in 20 mL of stirred THF to which was then added a THF solution of $W(CO)_5$(THF) [generated from 1.40 g of $W(CO)_6$], and THF (200 mL) was slowly added. When the addition was complete, stirring was continued for an additional 24 h. THF was then removed under reduced pressure to give a solid material that was heated at 70 °C (300 mtorr) to remove unreacted $W(CO)_6$. The residue was then dissolved in a minimum amount of THF followed by addition of pentane to give a precipitate which was filtered off and dried under reduced pressure to give **8i** in quantitative yield (based on **8h**). Single crystals for X-ray analysis were grown by vapor diffusion of pentane into a dichloromethane solution of **8i**. Mp: 186 °C. IR (Nujol, cm^{-1}): ν_{CO} 2071(s), 1977 (sh, s), 1942 (br, vs), 1906 (br, vs). $^{31}P\{^1H\}$ NMR ($CDCl_3$): δ −1.7 (d, $^1J_{WP}$ 91.2 Hz, PC_3),111.3 (d, $^1J_{WP}$ 170.9 Hz, PN_3), $^3J_{PP}$ 65.1 Hz. ^1H NMR ($CDCl_3$): δ 2.99 (dd, $^3J_{PH}$ 13.68 Hz, $^4J_{PH}$ 1.56 Hz, NCH_3, 9H), 3.53 (d, $^2J_{PH}$ 4.68 Hz, NCH_2, 6H). $^{13}C\{^1H\}$ NMR ($CDCl_3$): δ 43.2 (d, $^2J_{PC}$ 8.42 Hz, NCH_3, 3C), 51.4 (dd, $^1J_{PC}$ 21.90 Hz, $^2J_{PC}$ 3.37 Hz, NCH_2, 3C), 195.0 (d, $^2J_{PC}$ 6.74 Hz, $^1J_{WC}$ 60.64 Hz, *cis*-CO on W bonded to PC_3 end, 4C), 196.5 (d, $^2J_{PC}$ 10.10 Hz, $^1J_{WC}$ 62.33 Hz, *cis*-CO on W bonded to PN_3 end, 4C), 197.5 (d, $^2J_{PC}$ 13.47 Hz, *trans*-CO on W bonded to PN_3 end, 1C), 198.1 (d, $^2J_{PC}$ 5.05 Hz, *trans*-CO on W bonded to PC_3 end, 1C). Anal. Calcd for $C_{16}H_{15}N_3O_{10}P_2W_2$: C, 22.91; H 1.80; N, 5.00. Found: C, 22.88/22.88; H, 1.88/1.80; N, 4.92/4.95.

***cis*/*trans*-$Mo(CO)_4[P(NMeCH_2)_3P{=}O]_2$ (8l).** To a solution of **8b** (0.44 g, 2.1 mmol) in $CHCl_3$ (10 mL) was slowly added a solution of $Mo(CO)_4$(NBD) (0.31 g, 1.0 mmol) in 10 mL of $CHCl_3$. Crystals of **8l** grew on the sides of the flask along with some decomposition products. The crystals were hand picked, washed with a minimum amount of $CHCl_3$, and vacuum-dried. Yield: 32%. Mp: 260 °C (subl). IR (Nujol, cm^{-1}): ν_{CO} 2029 (m), 2022 (m), 1924 (s), 1907 (s), 1889 (s), 1878 (s); $\nu_{P=O}$ 1377 (m). $^{31}P\{^1H\}$ NMR ($CDCl_3$): second-order AA′MM′ pattern, δ 37.8 (dt, PC_3), 131.5 (dt, PN_3); spacing between the two adjacent lines in an apparent doublet, 99.5 Hz; spacing between the two adjacent lines in an apparent triplet, 20.1 Hz. ^1H NMR ($CDCl_3$): δ 2.91 (dd, $^3J_{PH}$ 12.84 Hz, $^4J_{PH}$ 2.04 Hz, NCH_3, 18H), 3.38 (dd, $^2J_{PH}$ 9.24 Hz; $^3J_{PH}$ 3.96 Hz, NCH_2, 12H). Anal. Calcd for $C_{16}H_{30}N_6O_6P_4Mo$: C, 30.88; H, 4.86; N, 13.50. Found: C, 30.79/30.78; H, 4.94/4.91; N, 13.55/13.66.

***cis*-Mo(CO)$_4$[P(CH$_2$NPh)$_3$P]$_2$ (9b).** A solution of Mo(CO)$_4$(NBD) (0.230 g, 0.766 mmol) in CH_2Cl_2 (10 mL) was slowly added to a CH_2Cl_2 (10 mL) solution of **9a** (0.582 g, 1.54 mmol). The mixture was allowed to stir for 24 h, and then solvent was removed under reduced pressure to give a solid that was stirred with hexanes. The hexanes-insoluble material was filtered off and dried under reduced pressure to afford **9b** in 82% yield. Mp: 145 °C (subl). IR (Nujol, cm^{-1}): ν_{CO} 1950 (s), 1931 (s, sh), 1924 (s), 1893 (s). ^{31}P{^{1}H} NMR ($CDCl_3$): second-order AA′MM′ pattern, δ_P 14.9 (four-line pattern, *P*C$_3$, 2P), 53.7 (four-line pattern, *P*N$_3$, 2P); spacing between two adjacent lines in the four line pattern, 5.50 Hz. ^{1}H NMR ($CDCl_3$): δ 3.86 (s, NC*H*$_2$, 12 H), 6.98, 7.25 (m, C$_6$*H*$_5$, 30H). Anal. Calcd for $C_{46}H_{42}N_6O_4P_2Mo{\cdot}CH_2Cl_2$: C, 53.88; H, 4.23; N, 8.02. Found: C, 53.42/52.42; H, 4.47/4.62; N, 8.03/7.93.

Reaction of 9a with Mo(CO)$_4$(NBD) (1:1 Ratio). The reaction of **9a** (0.179 g, 0.474 mmol) with 1 equiv of Mo(CO)$_4$(NBD) (0.142 g, 0.474 mmol) in CH_2Cl_2 at room temperature or with 1 equiv of Mo(CO)$_6$ (0.124 g, 0.470 mmol) in refluxing toluene for 12 h formed **9b** as shown by ^{31}P NMR spectroscopy.

Reaction of 9b with ClAu(SMe$_2$) (1:1 Ratio). To a suspension of ClAu(SMe$_2$) (0.294 g, 1.00 mmol) in $CHCl_3$ (8 mL) at room temperature was added a solution of **9b** (0.963 g, 1.00 mmol) in $CHCl_3$ (7 mL) over a period of 5 min. After stirring of the sample for an additional 24 h at room temperature, the ^{31}P NMR spectrum of the reaction mixture showed four broad resonances that are tentatively assigned to **9c**. ^{31}P{^{1}H} NMR($CDCl_3$): δ 14.7 (br, P$_A$), 38.6 (br, P$_{A'}$), 54.1 (br, P$_M$), 73.8 (br, P$_{M'}$).

Reaction of 9b with ClAu(SMe$_2$)(1:2 Ratio). To a suspension of ClAu(SMe$_2$) (0.294 g, 1.00 mmol) in chloroform (8 mL) at room temperature was added a solution of **9b** (0.481 g, 0.500 mmol) in chloroform (7 mL) over a period of 5 min. After being stirred for an additional 2 h at room temperature, the reaction mixture was filtered. The filtrate was concentrated to ca. 5 mL followed by the addition of Et_2O to obtain a brown solid which was washed with diethyl ether and dried under vacuum for 10 h to give **9d**. Single crystals for X-ray analysis were obtained by slow diffusion of Et_2O into a $CHCl_3$ solution of **9d**. ^{31}P{^{1}H} NMR(DMSO-d_6): second-order AA′MM′ pattern, δ 33.9 (four-line pattern, *P*C$_3$, 2P), 71.3 (four-line pattern, *P*N$_3$, 2P); spacing between two adjacent lines in the four-line pattern, 10.4 Hz. ^{1}H NMR (DMSO-d_6): δ 4.24 (br, NC*H*$_2$, 12H), 7.42 (m, C$_6$*H*$_5$, 30H). The DMSO or the DMF solution of **9d** upon standing became green and finally blue, suggesting oxidation of molybdenum. Elemental analysis could not be obtained for **9d** because of its high sensitivity to air, moisture, and light.

***fac*-Mo(CO)$_3$[P(CH$_2$NPh)$_3$P]$_3$ (9e).** A solution of Mo(CO)$_3$(CHT) (0.034 g, 0.125 mmol) dissolved in CH_2Cl_2 (5 mL) was added to **9a** (0.141 g, 0.375 mmol) dissolved in CH_2Cl_2 (10 mL). The mixture was stirred for 12 h, and then solvent and volatiles were removed under reduced pressure to give a solid which was dissolved in a minimum volume of CH_2Cl_2 and stored at room temperature for several days to obtain crystals of **9e**. Crystals were separated by hand, washed with hexanes, and dried under reduced pressure to give **9e** in 76% yield. Mp: 225 °C (dec). IR (Nujol, cm^{-1}): ν_{CO} 1943 (br, s), 1857 (s, br), 1844 (s). ^{31}P{^{1}H} NMR ($CDCl_3$): δ 14.1 (br, *P*C$_3$, 3P), 53.7 (br, *P*N$_3$, 3P). ^{1}H NMR ($CDCl_3$): δ 3.84 (s, NC*H*$_2$, 18H), 6.96, 7.24 (m, C$_6$*H*$_5$, 45H). Anal. Calcd for $C_{66}H_{63}N_9O_3P_6Mo$: C, 60.42; H, 4.84; N, 9.61. Found: C, 60.16/60.11; H, 5.19/5.23; N, 9.43/9.36.

(η^5-C$_5$Me$_5$)RuCl[P(CH$_2$NPh)$_3$P]$_2$ (9f). (η^5-C$_5$Me$_5$)Ru(COD)Cl (0.174 g, 0.458 mmol) and **9a** (0.301 g, 0.798 mmol) were charged to a Schlenk flask previously purged with nitrogen. To this was added CH_2Cl_2 (5 mL), and then the mixture was stirred for 12 h. Volatiles were removed under reduced pressure to give a residue that was dissolved in THF (10 mL) and filtered through a Celite pad. The filtrate was cooled to 0 °C for 12 h to give **9f** as an orange powder in 43% yield. Crystals were grown by vapor diffusion of pentane into a THF solution of **9f**. Mp: 248−250 °C (subl). ^{31}P{^{1}H} NMR ($CDCl_3$): δ 29.1 (br, *P*C$_3$, 2P), 55.3 (br, *P*N$_3$, 2P). ^{1}H NMR ($CDCl_3$): δ 1.82 (s, C$_5$(C*H*$_3$)$_5$, 15H), 3.87 (m, NC*H*$_2$, 12H), 6.95, 7.24 (m, C$_6$*H*$_5$, 30H). ^{13}C{^{1}H} NMR ($CDCl_3$): δ 11.7 (s, C$_5$(*C*H$_3$)$_5$, 5C), 44.8 (apparent t, $^1J_{PC}$, $^2J_{PC}$ 11.18 Hz, NC*H*$_2$, 6C), 90.9 (s, *C*$_5$(CH$_3$)$_5$, 5C), 116.3, 116.5, 120.9, 129.5, 147.9, 148.1 (s, *C*$_6$H$_5$, 36C). Anal. Calcd for $C_{52}H_{57}N_6P_4ClRu$: C, 60.84; H, 5.60; N, 8.19. Found: C, 60.59/60.41; H, 5.96/5.93; N, 8.26/8.20.

X-ray Structure Determinations. Crystals suitable for X-ray analysis were selected at room temperature, and air-sensitive samples were selected from under a layer of solvent. All samples were immediately covered with premixed epoxy glue to prevent decomposition. For low-temperature experiments, samples were immediately mounted and centered in the X-ray beam under a stream of cold nitrogen with the aid of a video camera.

Crystal evaluation and data collection were performed on a Bruker CCD-1000 diffractometer with Mo Kα (λ = 0.710 73 Å, graphite monochromator) radiation and a detector-to-crystal distance of 5.03 cm. Three series of ω scans at different starting angles were obtained to analyze the reflection profiles and to estimate the exposure time for data collection. Each series consisted of 30 frames collected at intervals of 0.3° in a 10° range about ω with an exposure time of 10−40 s/frame. Data were obtained using a full sphere routine by harvesting four sets of frames with 0.3° scans in ω with an exposure time 10−30 s/frame. The dataset was integrated with SMART software and analyzed with RLATT[25] software to separate the reflections belonging to one crystalline form for further calculations. Those datasets were corrected for Lorentz and polarization effects. The absorption correction was based on fitting a function to the empirical transmission surface as sampled by multiple equivalent measurements using SADABS software.[26]

The positions of some core non-hydrogen atoms for all the structures were found by direct methods. The remaining atoms were located in an alternating series of least-squares cycles and difference Fourier maps using SHELX[27] software. All non-hydrogen atoms were refined in a full-matrix anisotropic approximation. Typically all other hydrogen atoms were placed in the structure factor calculation at idealized positions and were allowed to ride on the neighboring atoms with relative isotropic displacement coefficients.

Structure 3a: colorless prism obtained by sublimation (0.40 × 0.420 × 0.30 mm); $C_3H_6O_3P_2$, M = 152.02; orthorhombic at 173 K, space group $Pnm2_1$; a = 8.389(2), b = 5.780(2), c = 6.420(2) Å; Z = 2, V = 311.33(14) Å^3; R1 = 0.0307, wR2 = 0.0702, GOF = 1.084.

Structure 8b: colorless block (0.40 × 0.40 × 0.30); $C_6H_{15}N_3OP_2$, M = 207.15; trigonal at 173 K, space group $P\bar{3}$; a = 7.2702(11), b = 7.2702(11), c = 10.952(2) Å; Z = 2, V = 501.32(14) Å^3; R1 = 0.0401, wR2 = 0.1072, GOF = 1.108.

Structure 8f: colorless plate (0.5 × 0.43 × 0.38); $C_6H_{21}B_2N_3P_2$, M = 218.82; orthorhombic at 173 K, space group *Pbca*; a = 13.0587(8), b = 13.2830(8), c = 14.2394(8) Å; Z = 8, V = 2469.9(3) Å^3; R1 = 0.0353, wR2 = 0.1061, GOF = 1.061.

Structure 8i: yellow prism (0.20 × 0.20 × 0.15); $C_{16}H_{15}N_3O_{10}P_2W_2$, M = 838.95; orthorhombic at 293 K, space group $Pca2_1$; a = 14.4369(8), b = 12.5461(7), c = 13.4794(7) Å; Z = 4, V = 2441.5(2) Å^3; R1 = 0.0226, wR2 = 0.0560, GOF = 1.053.

(26) Blessing, R. H. *Acta Crystallogr.* **1995**, *A51*, 33.
(27) All software and sources of the scattering factors are contained in the SHELXTL (version 5.1) program library (G. Sheldrick, Bruker Analytical X-ray Systems, Madison, WI).

Table 1. Comparison of Pertinent Structural Parameters of **8b**,**f**,**i** and **9a**,**d**,**e**,**f**[a]

params	8b	8f	8i	9a	9d	9e	9f
			Distances (Å)				
M−PC_3[b]		1.906(2)[c]	2.469(2)		2.4741(14) 2.4590(14)	2.4768(6) 2.4958(6) 2.4896(6)	2.2694(12) 2.2830(11)
M−PN_3[b]		1.893(2)[c]	2.520(2)		2.2075(13) 2.2121(13)		
P−C_{avg}	1.801(3)[d]	1.826(2)	1.80(2)	1.8358(l6)	1.843(5) 1.852(5)	1.835(2) 1.844(2) 1.837(2)	1.842(4) 1.841(4)
P−N_{avg}	1.7069(19)[d]	1.6663(15)	1.645(10)	1.7091(13)	1.677(4) 1.675(4)	1.711(2) 1.714(2) 1.709(2)	1.712(4) 1.714(4)
C−N_{avg}	1.471(4)[d]	1.478(2)	1.65(3)	1.4738(19)	1.481(6) 1.482(6)	1.458(3) 1.467(3) 1.466(3)	1.473(5) 1.468(5)
P···P	3.016(2)	2.9646(7)	3.062(3)	3.1310(5)	3.059(2) 3.052(2)	3.094(1) 3.110(1) 3.098(1)	3.126(2) 3.123(2)
			Angles (deg)				
NPN_{avg}	101.31(8)[d]	104.41(7)	98.6(8)	99.30(6)	102.0(2) 102.2(2)	100.33(10) 99.31(10) 100.26(9)	98.50(18) 99.23(18)
CPC_{avg}	102.38(12)[d]	101.00(9)	100.5(1)	97.80(7)	97.6(2) 98.0(2)	99.70(11) 98.82(11) 99.98(10)	97.9(2) 98.3(2)
PNC_{avg}	120.13(17)[d]	117.2(1)	112.7(1)	118.79(10)	115.9(3) 116.4(3)	120.8(2) 119.4(2) 121.2(2)	118.5(3) 119.2(3)
angle sums around N	351.4	347.2 353.8 353.5	354.5 351.1 350.0	358.2 358.8 357.7	358.9 355.4 358.2 356.7 359.9 359.9	358.5 360.0 359.7 358.1 359.1 356.2 360.0 360.0 359.8	356.2 358.3 359.9 354.7 355.0 359.9

[a] Analogous data for **3a** are as follows: P−C_{avg}, 1.844(3) Å; P−O_{avg}, 1.611(3) Å; C−O_{avg}, 1.453(4) Å; P···P, 3.082(4) Å; PCO_{avg}, 114.2(2)°; CPC_{avg}, 97.06(14)°; OPO_{avge} 102.07(13)°; P−O−C_{avg}, 122.15(17)°. [b] M indicates metal unless stated otherwise. [c] M indicates boron. [d] Not an average value because of crystallographic symmetry in the molecule.

Structure 9a: colorless prism (0.50 × 0.30 × 0.20 mm); $C_{21}H_{21}N_3P_2$, M = 377.35; monoclinic at 293 K, space group $P2_1/n$; a = 10.2430(4), b = 18.6675(8), c = 10.5701(4) Å; β = 109.5599(10)°; Z = 4, V = 1904.49(13) Å^3; R1 = 0.0326, wR2 = 0.0993, GOF = 1.039.

Structure 9d: colorless block (0.40 × 0.30 × 0.2); $C_{46}H_{42}Au_2Cl_2MoN_6O_4P_4$, M = 1427.51; monoclinic at 173 K, space group $P2_1/c$; a = 16.0152(8), b = 16.5984(8), c = 18.2588(9) Å; β = 92.0129(10)°; Z = 2, V = 4850.7(4) Å^3; R1 = 0.0304, wR2 = 0.0556, GOF = 1.007.

Structure 9e: colorless air-sensitive block (0.4 × 0.3 × 0.3); $C_{66}H_{63}MoN_9O_3P_6$, M = 1312.01; triclinic at 173 K, space group $P\bar{1}$; a = 13.7683(7), b = 16.2735(8), c = 16.8700(9) Å; α = 78.9063(10), β = 89.3240(10), γ = 87.4580(10)°; Z = 2, V = 3705.6(3) Å^3; R1 = 0.0393, wR2 = 0.0925, GOF = 1.017.

Structure 9f: orange prism (0.40 × 0.20 × 0.20); $C_{64}H_{69}ClN_6O_3P_2Ru$, M = 1230.65; monoclinic at 298 K, space group $P2_1/n$; a = 21.617(3), b = 12.1196(17), c = 25.563(4) Å; β = 109.264(2)°; Z = 4, V = 6322.4(15) Å^3; R1 = 0.0398, wR2 = 0.1127, GOF = 0.949.

Selected molecular geometrical parameters are summarized in Table 1.

Tolman Cone Angles. Using structural parameters obtained from the molecular structures of **3a**, **8b**,**f**,**i**, and **9a**,**d**,**e**,**f**, the Tolman cone angles around the phosphorus atoms in each were calculated, using 1.2 Å as the van der Waals radius of hydrogen, according to a literature method.[28] Structural parameters were obtained from molecular structures using the Ghemical-GMS[29] molecule building graphics program, and the data were processed using Microsoft Excel.[30] The Tolman cone angles were calculated by using a geometrically optimized hydrogen atom inserted in place of exocyclic atoms or lone pairs present on phosphorus atoms in **3a**, **8b**,**f**,**i**, and **9a**,**d**,**e**,**f** to represent a generalized metal atom (M) with an M−P bond length set to 2.28 Å as originally proposed by Tolman[31] (see Table 2). Tolman cone angles for the molecular structure of $Me_3P{=}O$[32] (121.07°), **14a** (113.76°),[33] and **14b** (112.97°)[34] were calculated from data obtained from the Cambridge Crystallographic Database.

(28) Mingos, D. M. P.; Müller, T. E. *Transition Met. Chem.* **1995**, *20*, 533−539.
(29) Acton, A.; Banck, M.; Bréfort, J.; Cruz, M.; Curtis, D.; Hassinen, T.; Heikkilä, V.; Hutchison, G.; Huuskonen, J.; Jensen, J.; Liboska, R.; Rowley, C. *Ghemical-GMS 1.01.06*; University of Iowa, Iowa City, IA, 1998−2003.
(30) Microsoft Office Excel 2003 SP2(US), Microsoft, Seattle, WA, 1985−2003.
(31) Tolman, C. A. *Chem. Rev.* **1977**, *77*, 313−348.
(32) Engelhardt, L. M.; Raston, C. L.; Whitaker, C. R.; White, A. H. *Aust. J. Chem.* **1986**, *39*, 2151−2154.
(33) Fluck, E.; Förster, J.; Weidlein, J.; Hadicke, E. *Z. Naturforsch.* **1977**, *32B*, 499−506.
(34) Darensbourg, D. J.; Yarbrough, J. C.; Lewis, S. J. *Organometallics* **2003**, *22*, 2050−2056.

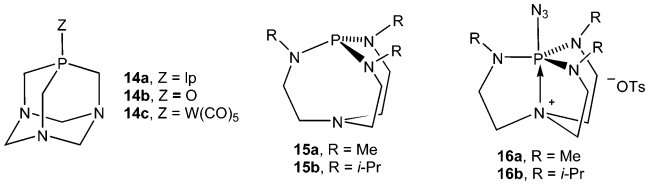

Results and Discussion

Compound 8a and Its Non-Metal Derivatives 8b−g. The reaction of P[(CH$_2$OH)$_4$]$_2$SO$_4$ with excess aqueous methylamine in water gave a mixture containing aminophosphine oligomers and a low conversion to P(CH$_2$NHMe)$_3$, the starting material for **8a**. Although a similar result has been reported for the reaction of P(CH$_2$OH)$_3$ with ammonia or primary amines,[24,35] P(CH$_2$NHCH$_2$COOH)$_3$ was obtained in 82% yield in such a reaction with glycine in water at pH 3−5.[36] Attempts to purify the crude P(CH$_2$NHMe)$_3$ by vacuum distillation led to decomposition. Therefore, it was characterized as **8a**, whose synthesis was accomplished in 25% overall yield by transaminating the P(CH$_2$NHMe)$_3$/aminophosphine oligomers with P(NMe$_2$)$_3$. Compound **8a** is a nonviscous liquid (stable to moisture and air for short periods) which slowly oxidizes in the atmosphere to afford the monoxide **8b**. Compound **8b** can be more efficiently prepared (in 53% yield) by reacting **8a** with excess activated MnO$_2$ under refluxing conditions, under which excess MnO$_2$ did not oxidize the PN$_3$ phosphorus of **8a**.

The reaction of **8a** with excess elemental sulfur in refluxing benzene gave a complex mixture from which the disulfide **8c** was isolated in 30% yield. While **8a** with 1 equiv of *p*-toluene sulfonyl azide also gave a complex mixture, the same reaction with 2 equiv produced **8d** in quantitative yield. By contrast, the reaction of *p*-toluenesulfonyl azide with the proazaphosphatranes (**15a**,**b)** afforded the corresponding azido proazaphosphatranes **(16a**,**b)**.[25] This result can be rationalized by the unusually sterically congested and electron rich nature of the PN$_3$ phosphorus in **(15a**,**b)** compared with the analogous phosphorus in **8a**.[25]

Interestingly, the PN$_3$ phosphorus of **8a** reacts with 1 equiv of BH$_3$·THF to give the monoadduct **8e** in 69% yield and the same reaction with 2 equiv of H$_3$B·THF furnished the diadduct **8f** in 40% yield. Diadduct **8f** upon treatment with 1 equiv of piperidine at room temperature gave the monoadduct **8e** in quantitative conversion after 2 h as revealed by ^{31}P NMR spectroscopy. However, the BH$_3$ group from the monoadduct **8e** was removed only with difficulty to give **8a**. Thus, **8f** upon treatment with 4 equiv of piperidine at 100 °C afforded **8a** after 15 h, along with small amounts of decomposition products. This displacement experiment suggests that the B←PN$_3$ bond in **8f** is stronger than the B←PC$_3$ bond. To the extent that P−B spin−spin coupling correlates with P−B bond strength,[37] the higher value of $^1J_{PB}$ for H$_3$B·P(NMe$_2$)$_3$ (variously reported as 95.0, 96.0, or 98.0 Hz)[38−40] and for **8e** (87.2 Hz) compared with that displayed by H$_3$B·PMe$_3$ ($^1J_{PB}$ = 59.8 Hz)[39] also suggests that the B←PN$_3$ bond is stronger than the B←PC$_3$ linkage. It appears that perhaps, despite steric pressure from the N−Me groups in **8e**, the B←PN$_3$ bond is favored over the B←PC$_3$ linkage by the electron richness of the phosphorus in the former owing to electron induction from the nitrogen lone pairs into the phosphorus.

Table 2. Tolman Cone Angles of PC$_3$, PN$_3$, or PO$_3$ Moieties in the Compounds Investigated

entry	compd	cone angle PC$_3$ (deg)	cone angle PN$_3$ or PO$_3$ (deg)
1	**3a**	112.46	106.00
2	**8b**	117.46	163.72
3	**8f**	120.14	168.56
4	**8i**	123.44	155.00
5	**9a**	118.96	214.24
6	**9d**	119.74	196.06
7	**9e**	118.70	228.34
8	**9f**	119.34	219.66

[a] All cone angles were measured from an H atom geometrically optimized and constrained to a bond distance of 2.28 Å from the phosphorus atom.

It has been suggested that the enthalpy of reaction for adduct formation of P(XYZ) (X, Y, Z = alkyl, alkoxy, Me$_2$N) with B$_2$H$_6$ is a reliable measure of the thermodynamic stability of the P−B bond in (XYZ)P·BH$_3$ adducts but that $^1J_{PB}$ is not.[41] Although our experiments with piperidine in the displacement of BH$_3$ from **8e**,**f** may be taken to indicate that the thermodynamic stability of the P−B bond does follow $^1J_{PB}$ in these particular compounds, it should be noted that enthalpies measured for the reaction of B$_2$H$_6$ with PMe$_3$ and with P(NMe$_2$)$_3$ are within 0.4 kcal/mol of one another (49.9 and 49.53 kcal/mol, respectively)[41] thus rendering any conclusions on these issues tenuous at best. We observed previously that the reaction of **3a** with B$_2$H$_6$ initially produced BH$_3$·P(CH$_2$O)$_3$P before proceeding to **3h**,[7] and it may be that, like **3a**, **8a** also initially reacts with 1 equiv of BH$_3$·THF to form BH$_3$·P(CH$_2$NMe)$_3$P before rapidly isomerizing to **8e**. This hypothesis is supported by the reaction of **8a** with 1 equiv of 9-BBN to furnish **8g**, a reaction that did not go to completion because **8a**,**g** formed an equilibrium mixture that prevented isolation of **8g**. The equilibrium between **8a** and **8g** may be attributable to steric interactions between the methyl groups of **8a** and the 9-BBN molecule.

IR and NMR Spectroscopic Studies of 8a−f. The ^{31}P NMR spectrum of the mixture of P(CH$_2$NHMe)$_3$ and aminophosphine oligomers showed a broad peak at −59.9 ppm which is in the expected range for compounds of the type P(CH$_2$NH−)$_3$.[17,24,36] The ^{31}P NMR spectrum of **8a** displayed an AM pattern consisting of a pair of doublets due to mutual coupling of the two chemically different phosphorus atoms.[6c,17] The ^{31}P chemical shift for the PN$_3$ phosphorus in **8a** (82.3 ppm) is upfield relative to that for

(35) Daigle, D. J.; Frank, A. W. *Text. Res. J.* **1982**, *52*, 751−755.
(36) Berning, D. E.; Katti, K. V.; Barnes, C. L.; Volkert, W. A. *J Am. Chem. Soc.* **1999**, *121*, 1658−1664.
(37) Rudolph, R. W.; Schultz, C. W. *J. Am. Chem. Soc.* **1971**, *93*, 6821−6822.
(38) Noth, H.; Vahrenkamp, H. *Chem. Ber.* **1966**, *99*, 1049−1067.
(39) Cowley, A. H.; Damasco, M. C. *J. Am. Chem. Soc.* **1971**, *93*, 6815−6821.
(40) Wrackmeyer, B. Z. *Naturforsch., B* **1984**, *39*, 533−534.
(41) Jugie, G.; Jouany, C.; Elegant, L.; Gal. J. F.; Azzaro, M. *Bull. Soc. Chim. Fr.* **1976**, (1−2), part 1, 1−4.

$P(NMe_2)_3$ (δ_P 123.0 ppm[42]). We are unable to associate this upfield shift with a significant change in the average NPN angle in **8a** {which is probably close to those in **9a** [99.30(6)°] and **8b** [101.31(8)°] (see below)} relative to that in $P(NMe_2)_3$ [average NPN angle = 102.0(2)°[43]]. A similar upfield shift for **17a** (δ_P 83.5 ppm) was reported on the basis of a presumed decrease in the NPN angles relative to $P(NMe_2)_3$[44] and for **18** (δ_P 22.3 ppm) relative to **19** (δ_P 64.8 ppm).[45]

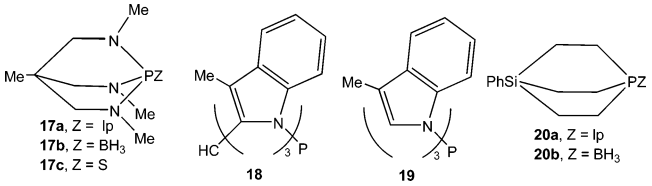

The δ_P value for the PC_3 phosphorus in **8a** (δ_P −53.1 ppm) is shifted downfield relative to acyclic PMe_3 (δ_P −62.0 ppm)[42] and **20a** (δ_P −59.2 ppm).[46] The CPC angle in PMe_3 [calculationally optimized average CPC angle = 99.4°;[47] X-ray diffractionally determined CPC angle = 99.1(1)−99.4(1)°;[48] electron diffractionally determined average CPC angle = 98.6(3)°[49]] are all within 1° of that in **9a** [average CPC angle = 97.80(7)° (see below)].

The average CPC angle in **20a** is 100.9°.[46] It therefore appears that more subtle effects are responsible for these shift differences than small changes in bond angles. Thus, for example, the average CPC angle in **14a** [96.1(1)°][33] is within experimental error of that in **9a** and yet the δ_P for the PC_3 phosphorus in **14a** (−98.3 ppm)[50] is ca. 53.0 ppm further upfield of that in **9a** (−45.3 ppm[6c,17]). The δ_P value for the PC_3 phosphorus in **8a** (−53.1 ppm) is shifted upfield by only 7.8 ppm relative to that in **9a** (−45.3 ppm[6c,17]) while that of the PN_3 phosphorus in **8a** (82.3 ppm) is significantly shifted downfield by 32.6 ppm from the corresponding phosphorus in **9a** (49.7 ppm[6c,17]), indicating considerable sensitivity of the chemical shifts of the PN_3 phosphorus to the influence of the orientation and the nature of the carbon substituents and of the lone pairs on the nitrogens.

The ^{31}P NMR spectra of **8c**,**d** also consisted of pairs of doublets with δ_P values corresponding to the PC_3 phosphorus in each case appearing significantly downfield relative to that in **8a**, while those of the PN_3 phosphorus in both compounds appear at relatively high field. These results are consistent with the reported relative δ_P values between $P(NMe_2)_3$ and $S{=}P(NMe_2)_3$,[42] between **11** and the disulfide of **11**,[19a,19b,51] between PMe_3 and $S{=}PMe_3$,[42] and between **17a** and **17c**.[44,51] Interestingly, $^3J_{PP}$ values of 107.8 and 115.1 for **8c**,**d**, respectively, are comparable to those reported for **8j** (116.6 Hz) and **8k** (114.6 Hz)[25] but are significantly higher than that observed for **8a** ($^2J_{PP}$ 26.6 Hz).

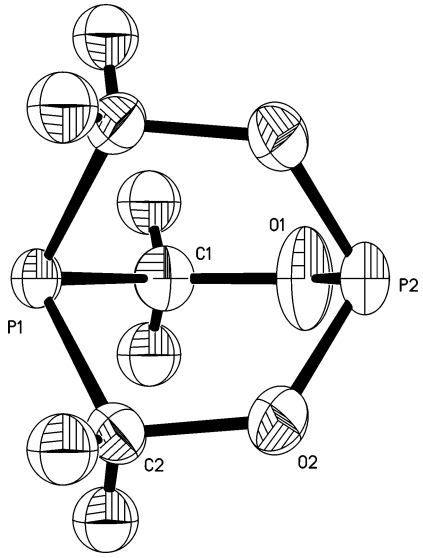

Figure 1. ORTEP view of structure **3a** at the 50% probability level.

The ^{31}P NMR spectrum of **8e** showed a doublet for the PC_3 phosphorus with an unusually low $^{31}P-^{31}P$ spin−spin coupling (8.6 Hz) and four equally intense lines for the PN_3 phosphorus due to coupling with the ^{11}B ($I = 3/2$) nucleus ($^1J_{PB}$ = 88.5 Hz). Binding of the BH_3 moiety to the PN_3 phosphorus in **8e** is consistent with its ^{11}B NMR spectrum that features a doublet centered at −43.4 ppm ($^1J_{PB}$ 87.2 Hz) lying very close to the ^{11}B NMR chemical shifts (−45 ± 5 ppm) recorded for phosphine−borane adducts.[52]

The $^1J_{PB}$ value of 88.5 Hz for **8e** is greater than that reported for **17b** ($^1J_{PB}$ = 77.0 Hz)[19c] but smaller than those reported for $H_3B{\cdot}P(NMe_2)_3$ (variously reported as $^1J_{PB}$ = 95.0, 96.0, and 98.0 Hz)[38−40] and the BH_3 adduct of **15a** ($^1J_{PB}$ 109.0 Hz).[53] To the extent that the values of $^1J_{PB}$ for these monoadducts can be correlated with the dative P−B bond strength,[37] the order **17b** < **8e** < $H_3B{\cdot}P(NMe_2)_3$ < **15a**·BH_3 emerges, which is consistent with an increasing order of Lewis basicity for the PN_3 phosphorus in the order **17a** < **8a** < $P(NMe_2)_3$ < **15a**.

X-ray Structure Analyses of 3a, 9a, and 8b,f. Computer drawings of the molecular structures for these compounds are shown in Figures 1−4, respectively. The nonbonded P···P distance, 3.082(4) Å in **3a** (Figure 1), is slightly shorter than that reported for **4a** [3.132(1) Å].[14] The greater length of this distance in **3a** than those reported for **3f** [2.994(3) Å],[8] **3u** [3.025(5) and 3.022(5) Å for the PO_3 and the PC_3 phosphorus-coordinated ligands, respectively],[11] and P[C{-

(42) Tebby, J. C. *Handbook of Phosphorus-31 Nuclear Resonance Data*; CRC Press: Boca Raton, FL, 1991; Chapter 5, p 93, Chapter 6, p 121, and Chapter 9, p 227.
(43) Mitzel, N. W.; Smart, B. A.; Dreihäupl, K-H.; Rankin, D. W. H.; Schmidbaur, H. *J. Am. Chem. Soc.* **1996**, *118*, 12673−12682.
(44) Kroshefsky, R. D.; Verkade, J. G. *Inorg. Chem.* **1975**, *14*, 3090−3095.
(45) Barnard, T. S.; Mason, M. R. *Organometallics* **2001**, *20*, 206−214.
(46) Ochida, A.; Hara, K.; Ito, H.; Sawamura, M. *Org. Lett.* **2003**, *5*, 2671−2674.
(47) Suresh, C. H.; Koga, N. *Inorg. Chem.* **2002**, *41*, 1573−1578.
(48) Bruckmann, J.; Kruger, C. *Acta Crystallogr.* **1995**, *C51*, 1155−1158.
(49) Bartell, L. S. *J. Chem. Phys.* **1959**, *32*, 512−515.
(50) Daigle, D. *J. Inorg. Synth.* **1998**, *32*, 40−45.
(51) White, D. W.; Karcher, B. A.; Jacobson, R. A.; Verkade, J. G. *J. Am. Chem. Soc.* **1979**, *101*, 4921−4925.
(52) Brunel, J. M.; Faure, B.; Maffei, M. *Coord. Chem. Rev.* **1998**, *178−180*, 665−698.
(53) Gudat, D.; Lensink, C.; Schmidt, H.; Xi, S.-K.; Verkade, J. G. *Phosphorus, Sulfur, Silicon Relat. Elem.* **1989**, *41*, 21−30.

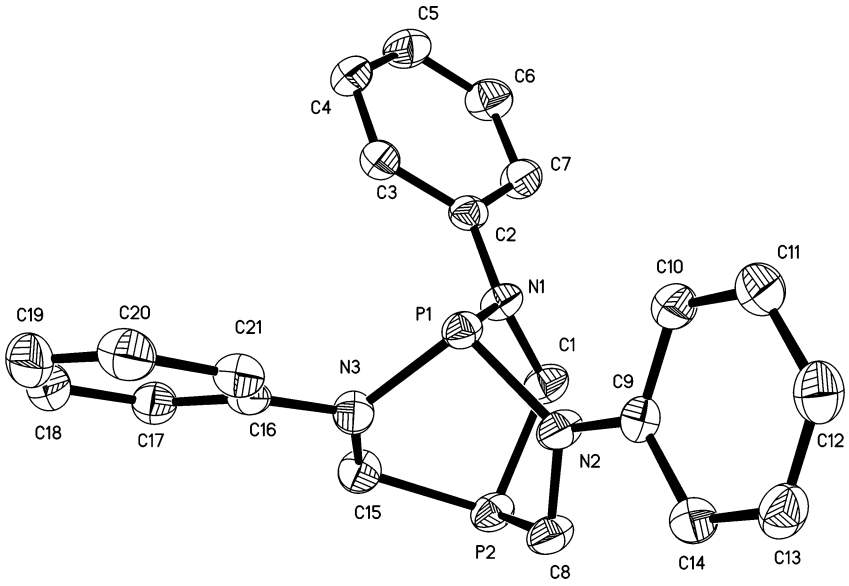

Figure 2. ORTEP view of structure **9a** at the 50% probability level. Hydrogen atoms are omitted for clarity.

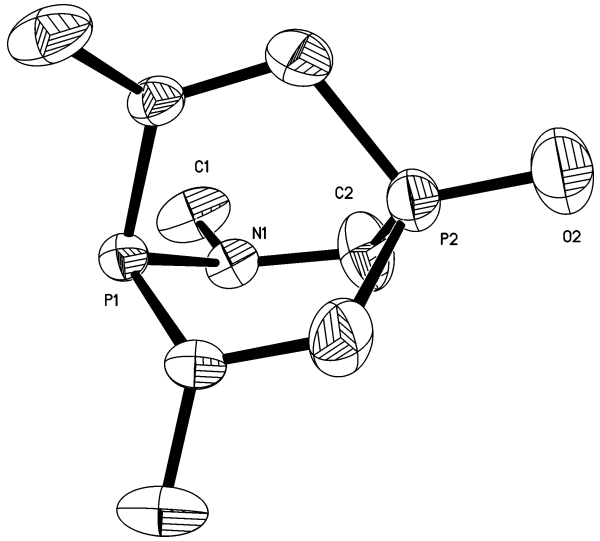

Figure 3. ORTEP view of structure **8b** at the 50% probability level. Hydrogen atoms are omitted for clarity.

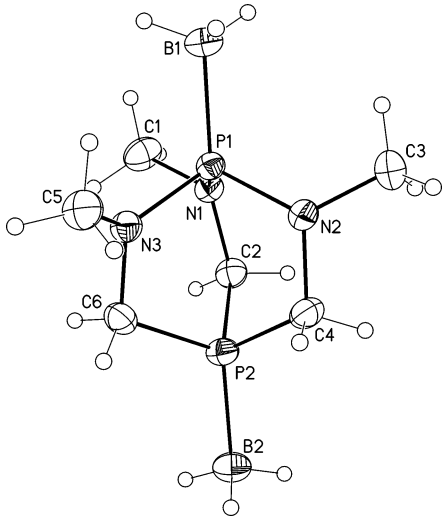

Figure 4. ORTEP view of structure **8f** at the 50% probability level showing atom numbering.

$(CF_2)_2H\}HO]_3P{=}O$ [3.036(3) Å][54] is made reasonable by the compression of this distance expected upon coordination/oxidation of phosphorus, which is expected to increase the angles inside the cage around the phosphorus. Thus, the average OPO angle in **3a** [102.07(13)°] enlarges in **3f** [106.1(2)°][8] and in the PO_3 phosphorus-coordinated ligand in **3u** [104.2(4)°].[11] The nonbonded P···P distances in **3a**, **3f**, P[C{-$(CF_2)_2H\}HO]_3P{=}O$, and **4** are shorter than the sum of the Van der Waals radii of 3.70 Å for two phosphorus atoms but longer than the normal P−P single bond of 2.21 Å.[55]

The P═O distance [1.485(4) Å] and CPC bond angle [102.38(12)°] in **8b** compare with 1.489(6) Å and 105.8(3)° in O═PMe$_3$, respectively,[32] and with 1.476(2) Å and 100.2(1)° in **14b**, respectively.[58] Although two different P−N bond lengths [1.683(3) and 1.732(3) Å] as well as two different angle sums around the nitrogens [336.7 and 356°][43] were reported for P(NMe$_2$)$_3$, all the P−N bonds in **8b** (Figure 3) are equal [1.706(19) Å] as are also the angle sums for all three nitrogens in **8b** (351.4°) owing to crystallographic symmetry. The nonbonded P···P distance in **8b** [3.016(2) Å] is shorter than that found in **9a** [3.1310(5) Å] owing to oxidation of one of the phosphorus atoms in the former (see below).

Unlike **8b** and **9a** (see below), the structure of **8f** (Figure 4) contains one P−N bond length that is somewhat longer [1.676(1) Å] than the others [1.661(2), 1.662(2) Å] as was also reported for H$_3$B·P(NMe$_2$)$_3$ [1.683(1), 1.658(1), and

(54) Zub, Y. L.; Skopenko, V. V.; Fundamenskii, V. S.; Markovskii, L. N.; Danchenko, E. A.; Shermolovich, Y. G. *Zh. Strukt. Khim.* **1987**, *28*, 163−165.
(55) Huheey, J. E.; Keiter, E. A.; Keiter, R. L. *Principles of Structure and Reactivity*, 4th ed.; Harper Collins College Publishers: New York, 1993; p 290.
(56) Van Doorne, W.; Hunt, G. W.; Parry, R. W.; Cordes, A. W. *Inorg. Chem.* **1971**, *10*, 2591−2594.
(57) Cordes, A. W.; Fair, C. K.; Bermann, M.; Van Wazer, J. R. *J. Cryst. Mol. Struct.* **1975**, *5*, 279−285.
(58) Jogun, K. H; Stezowski, J. J; Fluck, E; Weidlein J. *Phosphorus Sulfur* **1978**, *4*, 199−204.

1.650(1) Å].[59] The geometry of the nitrogens in **8f** also deviates significantly from planarity (angle sums = 347.2, 353.8, and 353.5°) as is also the case for $H_3B{\cdot}P(NMe_2)_3$ (angle sums = 343.1, 353.3, and 359.8°).[59] These distortions in trisaminophosphines have been ascribed to electron donation of the unhybridized p-orbital lone pairs on the two virtually planar nitrogens to the phosphorus.[60] The phosphorus electron density is thus "saturated" to the point where the nitrogen in the remaining longer bonded P−N linkage is free to adopt a pyramidal geometry normally associated with an amino nitrogen. Because of the bicyclic structure of **8f**, its reduced symmetry around the PN_3 phosphorus could be ascribed to crystallographic packing effects. The N_3P-B distance in **8f** [1.893(2) Å] is slightly shorter than that reported for $H_3B{\cdot}P(NMe_2)_3$ [1.913(1) Å],[59] and it is significantly shorter than that reported for **17b** [1.98(3) Å].[61] The C_3P-B distance in **8f** [1.906(2) Å] is comparable to that reported for $H_3B{\cdot}PMe_3$ [1.892 (7) Å][62] but smaller than that found in **20b** [1.922(2) Å].[46] The nonbonded P···P distance in **8f** [2.9646(7) Å] is significantly shorter than that observed for **9a** [3.1310(5) Å] and **8b** [3.016(2) Å], which can be associated with the opening of the NPN bond angle from **9a** and **8b** to **8f**.

The phenyls in **9a** (Figure 2) form a paddle wheel arrangement around the cage with the average P−N distance [1.7091(13) Å, Table 1], and the geometry of the nitrogens (angle sums = 358.3, 358.8, and 357.7°) closely resembles those in **18** [1.708(2) Å; 357.5, 359.8, and 360°].[45] The nonbonded P···P distance in **9a** [3.1310(5) Å], however, might appear to be longer than those found in **11** (2.99 Å),[56] in the diiminophenyl derivative of **11** (2.844 Å)[57] and in the dioxide of **11** (2.82 Å),[19e] although esd values could not be found for these derivatives of **11** for comparison.

Transition Metal Complexes of 8a,b and 9a. The PC_3 phosphorus of **8a** reacts with $W(CO)_5$(THF) in THF to give **8h** (48% yield) as the only product, in contrast to our earlier report of the reaction between $W(CO)_5$(aniline) and **3a** in 1:1 ratio that produced a mixture of **3n**,**q** in variable yield.[10] The uncoordinated PN_3 phosphorus of **8h** reacts with $W(CO)_5$(THF) in THF to afford **8i** in quantitative yield. The selectivity to give **8h** prior to forming **8i** may be associated with steric pressure from the methyl groups in **8a**.

The contrasting stereoselectivity in the reaction of **8a** with $BH_3{\cdot}$THF and with $W(CO)_5$(THF) deserves comment. Apparently the PN_3 phosphorus is more basic than the PC_3 phosphorus in **8a** because of the inductive effect of the 2p nitrogen lp on the planar nitrogen in each of the NMe groups. As a result, the PN_3 phosphorus in **8a** preferentially reacts with the soft Lewis acid $BH_3{\cdot}$THF to form the adduct **8e**, whereas the less sterically hindered PC_3 phosphorus of **8a** binds preferentially with the sterically crowded $W(CO)_5$ moiety (also a soft Lewis acid) to form **8h**. The IR spectrum of **8h** showed three ν_{CO} bands (2072, 1943, 1913 cm^{-1}) characteristic for $(OC)_5W(PR_3)$.[34,63] These values are lower than those for $(OC)_5W(PMe_3)$ (ν_{CO} 2073, 1952, 1942 cm^{-1} [63]) suggesting that the PC_3 phosphorus in **8a** may be a somewhat a better σ-donor/poorer π-acceptor than PMe_3. Two of the three IR frequencies for the CO groups in **8h** are lower than those for **14c** (2072, 1955, 1944 cm^{-1}).[34] The smaller $^1J_{WP}$ value of **8h** (118.0 Hz) than that for $(OC)_5W(PMe_3)$ (230 Hz)[64] and **14c** (218.2 Hz) is not readily interpretable in terms of relative bonding characteristics of the ligands. The CPC angle in **14c** [96.1(1)°][34] is smaller than that in **8i** [100.5(1)°, Table 1], and the W−P distance [2.4976(15) Å] in **14c** is slightly longer than in **8i** [2.469(2) Å] (see below).

The reaction of $Mo(CO)_4$(NBD) with 2 equiv of **9a** in CH_2Cl_2 produced **9b** in 82% yield. In the analogous reactions involving **3a** and group VI metal tetracarbonyl precursors, PO_3 phosphorus coordination was realized in **3w** whereas PC_3 phosphorus coordination was preferred in **9b**,**e**,**f** (see below). This difference is also easily rationalized on steric grounds. A reaction of equimolar quantities of $Mo(CO)_4$(NBD) and **9a** in CH_2Cl_2 at ambient temperature gave **9b** according to ^{31}P NMR spectroscopy instead of the intended square macrocycle *cyclo*-$\{Mo(CO)_4[P(CH_2NPh)_3P]\}_4$ analogous to rings of type **3v** realized with **3a**.[9] Further, a reaction of equimolar quantities of $Mo(CO)_6$ and **9a** in refluxing toluene for 12 h again produced **9b** as the only species detectable by ^{31}P NMR spectroscopy. The favored formation of cis-disubstituted **9b** under the latter conditions is quite remarkable, since we know of no report of the analogous reaction product being synthesized in a reaction of $M(CO)_6$ (M = Cr, Mo, W) with PMe_3, except after prior formation of a *cis*-$M(CO)_4$(diene) intermediate, as has long been known.[65a,65b] *cis*-$M(CO)_4(PMe_3)_2$ complexes (M = Mo, W) have been similarly synthesized by electrolysis of a mixture of $Mo(CO)_6$/THF followed by addition of PMe_3,[66] and *cis*-$Cr(CO)_4(PMe_3)_2$ has been made by electrolysis of $Cr(acac)_3$ in the presence of CO and PMe_3.[67] The favored formation of cis-disubstituted **9b** in refluxing toluene is also noteworthy because *cis*-$M(CO)_4(PMe_3)_2$ (M = Cr, Mo, W) readily isomerize to their respective trans isomers above 50 °C.[68] Three of the four CO stretching frequencies in **9b** (1950, 1931, 1924, 1893 cm^{-1}) are larger than those in *cis*-$Mo(CO)_4(PMe_3)_2$ [(2016, 1910, 1896, 1874 cm^{-1}),[65b] but only two of the four CO stretching frequencies in **9b** are larger than that recorded elsewhere for *cis*-$Mo(CO)_4[PMe_3]_2$ (2019,

(59) Mitzel, N. W.; Lustig, C. *J. Chem. Soc., Dalton Trans*. **1999**, 3177−3183.
(60) (a) Clarke, M. L.; Cole-Hamilton, D. J.; Slawin, A. M. Z.; Woollins, J. D. *Chem. Commun.* **2000**, 2065−2066. (b) Clarke, M. L.; Cole-Hamilton, D. J.; Woollins, J. D. *J. Chem. Soc., Dalton Trans.* **2001**, 2721−2723. (c) Kárpáti, T.; Veszprémi, T.; Thirupathi, N.; Liu, X. Wang, Z.; Ellern, A.; Nyulászi, L.; Verkade, J. G. *J. Am. Chem. Soc.* **2006**, *128*, 1500−1512.
(61) Clardy, J. C.; Kolpa, R. L.; Verkade, J. G. *Phosphorus* **1974**, *4*, 133−141.
(62) Ijima, K.; Hakamata, Y.; Nishikawa, T.; Shibata, S. *Bull. Chem. Soc. Jpn.* **1988**, *61*, 3033−3036.
(63) Cotton, F. A.; Darensbourg, D. J.; Kolthammer, B. W. S. *Inorg. Chem.* **1981**, *20*, 4440−4442.
(64) Stelzer, O.; Unger, E. *Chem. Ber.* **1975**, *108*, 1246−1258.
(65) (a) Mathieu, R.; Poilblanc, R. *C. R. Acad. Sci., Ser. C* **1967**, *264*, 1053−1056. (b) Jenkins, J. M.; Moss, J. R.; Shaw, B. L. *J. Chem. Soc. A* **1969**, 2796−2800.
(66) Grobe, J.; Zimmermann, H. *Z. Naturforsch., B: Anorg. Chem. Org. Chem.* **1981**, *36B*, 301−306.
(67) Grobe, J.; Zimmermann, H. *Z. Naturforsch., B: Anorg. Chem. Org. Chem.* **1980**, *35B*, 533−538.
(68) Apel, C., J.; Bacher, R.; Grobe, J.; Le Van, D. *Z. Anorg. Allg. Chem.* **1979**, *453*, 39−52.

1922, 1905, 1899 cm^{-1})].[69] These data do not permit any conclusion regarding the relative σ-donor/π-acceptor properties of **9a** versus PMe_3.

The reaction of **9b** with 1 equiv of $AuCl(Me_2S)$ in chloroform produced **9c** as shown by ^{31}P NMR spectroscopy, and the same reaction with 2 equiv of $AuCl(Me_2S)$ in chloroform for 2 h produced **9d**. Both **9c**,**d** are sensitive to air, moisture, and light, which precluded satisfactory elemental analyses.

The reaction of $Mo(CO)_4$(NBD) with 2 equiv of **8b** in $CHCl_3$ furnished a cis−trans mixture of **8l** in 32% yield. The IR spectrum of **8l** showed six well-separated CO bands (2029, 2022, 1924, 1907, 1889, 1878 cm^{-1}) which contrasts the three or four CO bands reported for *cis*-$Mo(CO)_4[P(NMe_2)_3]_2$,[64,70,71] the three CO bands (and sometimes one band) reported for *trans*-$Mo(CO)_4[P(NMe_2)_3]_2$,[19c] and the three (or sometimes two) CO bands reported for *trans*-$Mo(CO)_4[P(NMeCH_2)_3CMe]_2$.[19c] The observation of six CO bands for **8l** is consistent with a mixture of cis and trans isomers. It was previously found that *cis*-$Mo(CO)_4[P(NMe_2)_3]_2$ is stable in the solid state. However, this compound does isomerize to its trans isomer over 30 min in benzene at room temperature, although, interestingly, the more sterically hindered *cis*-$Mo(CO)_4[P(NMePh)_3]_2$ did not isomerize in toluene even after refluxing for 24 h.[70,72]

The reaction of $Mo(CO)_3$(CHT) with 3 equiv of **9a** in dichloromethane produced **9e** in 76% yield. Its *fac* coordination geometry (see below) is supported by the three CO frequencies in its IR spectrum (1943, 1857, 1844 cm^{-1}). The ν_{CO} values of **9e** are higher than those reported for *fac*-[$Mo(CO)_3(PMe_3)_3$] (1927, 1828 cm^{-1})[65b] and *fac*-[$Mo(CO)_3$(**14a**)$_3$] (1930, 1840 cm^{-1})[73] here indicating a poorer σ-donor/better π-acceptor nature of the PC_3 phosphorus in **9a** relative to PMe_3 and **14a** for reasons that are not clear. The reaction of (η^5-C_5Me_5)RuCl(COD) with **9a** in a 1:2 molar ratio in dichloromethane produced **9f** in 43% yield, and the same reaction in a 1:1 molar ratio also gave **9f** (as indicated by ^{31}P NMR spectroscopy) instead of the macrocycle *cyclo*-{-(η^5-C_5Me_5)RuCl[$P(CH_2NPh)_3P$]}$_6$. The structures of the products obtained from reactions of **9a** or **8a** with appropriate metal precursors suggest that the NR organic substituents in these diphosphorus cages do not favor cyclic oligomers because of interligand mutual steric interference in such structures, as space-filling models confirm.

X-ray Structure Analyses of 8i and 9d,e,f. The molecular structures of these compounds are shown in Figures 5−8, respectively, and parameters pertinent for comparisons among these molecules are listed in Table 1. The W−PC_3 distance of 2.469(2) Å in **8i** is shorter than that reported for $(OC)_5W(PMe_3)$ [W−P, 2.516(2) Å][63] and for **14c** [W−P, 2.4976(15) Å][34] providing further support of the greater σ-donor/poorer π-acceptor properties of the $P(CH_2CH_2NMe)_3PW(CO)_5$ ligand. The large standard deviation in the *trans*-W−C distance in **8i** prevented comparisons. The geometry around the molybdenum in **9d** (Figure 6) is close to octahedral, and that of each gold atom is almost linear [P(2)−Au(1)−Cl(1) = 173.82(5)°, P(4)−Au(2)−Cl(2) = 178.74(5)°]. The average Mo−PC_3 distance, 2.4665(14) Å, in **9d** is shorter, but the average *trans*-Mo−C distance of 1.998(5)Å is slightly longer in **9d** than that reported for *cis*-$Mo(CO)_4(PMe_3)_2$ [average Mo−P and average *trans*-Mo−C distances are 2.522(1) and 1.971(5) Å, respectively][69] a result which is also consistent with the greater σ-donor/poorer π-acceptor properties of **9a**. As a result of PN_3 coordination to gold, the average P−N distance [1.677(4), 1.675(4) Å in ligands 1 and 2, respectively] and the nonbonded P···P distances [3.059(2), 3.052(2) Å in ligands 1 and 2, respectively] in **9d** are shorter than those observed for **9a** [1.7091(13) and 3.1310(5) Å, respectively]. The average P−N distance in **9d** is slightly longer than that reported for $(Me_2N)_3PAuCl$ [average P−N = 1.65(1) Å].[74] The geometry of one of the three nitrogens in **9d** deviates slightly from planarity (angle sums = 355.4, 356.7° in ligands 1 and 2, respectively) while the other two nitrogens possess virtually planar geometries (angle sums = 358.9, 358.2° in ligand 1; 359.9, 359.9° in ligand 2].

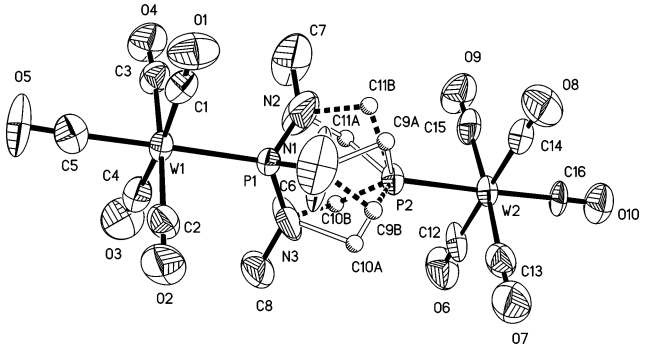

Figure 5. ORTEP view of structure **8i** at the 50% probability level. Hydrogen atoms are omitted for clarity. For the disordered positions of atoms thermal ellipsoids were substituted by a "ball" representation. "Disordered" positions are drawn with open and dashed lines.

The *fac* molybdenum complex **9e** features three PC_3 **9a** ligand moieties (Figure 7). The Mo−P and *trans*-Mo−C distances in **9e** [1.9857(3) and 2.4874(6) Å] differ significantly from the corresponding distances in *fac*-$Mo(CO)_3$(**14a**)$_3$ [1.964(8) and 2.494(3) Å].[73] The longer Mo−P and shorter *trans*-Mo−C distances in **9e** is consistent with the aforementioned conclusion based on ν_{CO} values that ligand **9a** is a poorer σ-donor/better π-acceptor than **14a**. The structure of **9f** (Figure 8) resembles the three-legged piano stool structure found for (η^5-C_5Me_5)RuCl(PMe_3)$_2$.[75] The average Ru−P distance in **9f** [2.2762(11) Å] is shorter than

(69) Cotton, F. A.; Darensbourg, D. J.; Klein, S.; Kolthammer, B. W. S. *Inorg. Chem.* **1982**, *21*, 2661−2666.
(70) Ogilvie, F. B.; Jenkins, J. M.; Verkade, J. G. *J. Am. Chem. Soc.* **1970**, *92*, 1916−1923.
(71) Ogilvie, F. B.; Keiter, R. L.; Wulfsberg, G.; Verkade, J. G. *Inorg. Chem.* **1969**, *8*, 2346−2349.
(72) King, R. B. *Inorg. Chem.* **1963**, *2*, 936−944.
(73) Alyea, E. C.; Ferguson, G.; Kannan, S, *Polyhedron* **1997**, *16*, 3533−37.
(74) Bauer, A.; Mitzel, N. W.; Schier, A.; Rankin, D. W. H.; Schmidbaur, H. *Chem. Ber./Recueil* **1997**, *130*, 323−328.
(75) Smith, D. C.; Haar, C. H.; Luo, L.; Li, C.; Cucullu, M. E.; Mahler, C. H.; Nolan, S. P. *Organometallics* **1999**, *18*, 2357−2361.

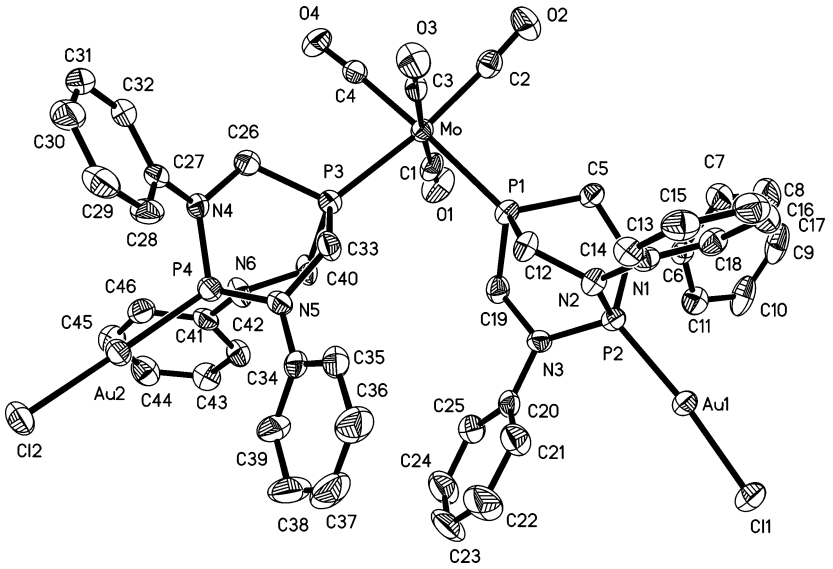

Figure 6. ORTEP view of structure **9d** at the 50% probability level. Hydrogen atoms are omitted for clarity.

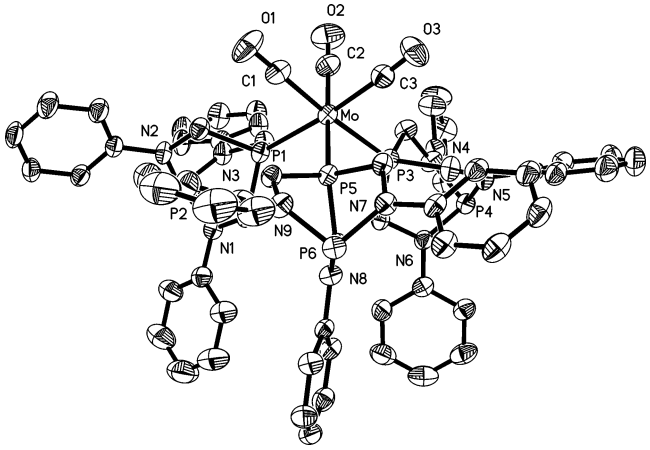

Figure 7. ORTEP view of structure **9e** at the 50% probability level. Hydrogen atoms are omitted for clarity.

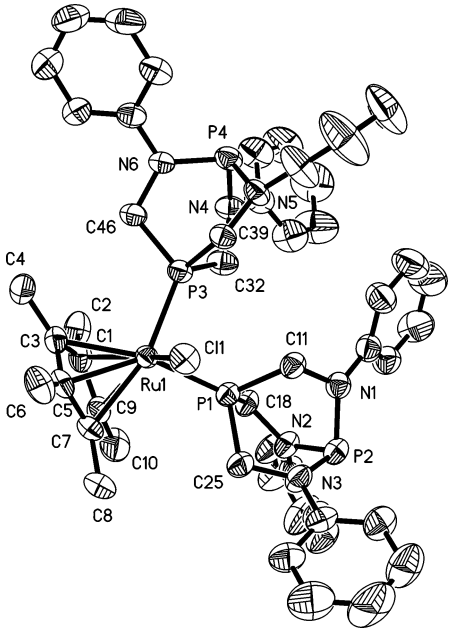

Figure 8. ORTEP view of structure **9f** at the 50% probability level. Hydrogen atoms are omitted for clarity.

that in (η^5-C_5Me_5)RuCl(PMe_3)$_2$ [average Ru−P = 2.2969(9) Å][75] and (η^5-C_5Me_5)RuCl(**14a**)$_2$ [average Ru−P = 2.2858(15) Å][76] a result that suggests better σ-donor/poorer π-acceptor properties of **9a** relative to PMe_3.

Tolman Cone Angles for 3a, 9a, 8b,f,i, and 9d,e,f. The Tolman cone angles for the PC_3, PO_3, and PN_3 moieties in Table 2 can be compared with those found in the literature for the analogous acyclic phosphorus ligands which are PMe_3 [118(4)° from CPK models;[31] 113(2)° from X-ray results;[48] 117° via MM2 calculations[77]], $P(OMe)_3$ [107(4)°[31])], and $P(NMe_2)_3$ [157(4)°[31]]. The X-ray-derived PC_3 cone angles for all the compounds in Table 2 except **8i** are within 3 × the esd of that for PMe_3. It is not clear why the PC_3 cone angle for **8i** is ca. 4° larger than the upper limit (119°) of the error range. Nonetheless, it is interesting that despite the changes in polarizing power of the Z groups on P in Table 2, these cone angles remain rather constant. Thus, despite the significant polarizing power of the oxygen ligand in **8b** (which opens the CPC angle via rehybridization) from 97.80(7)° in **9a** to 102.38(12)° in **8b**, the cone angles for their respective $ZP(CH_2)_3$ moieties are within 2° of one another. The effect on cone angle of the rehybridization effect is clearly seen in a comparison of PMe_3 with O═PMe_3, however, in which the cone angle increases from 113(2) in the former to 121.07° in the latter while the CPC bond angles increase from 99.1(11) and 99.4(1)° in the former to 105.8(3)° in the latter.[32] Due to constraint in the bicyclic framework, this effect is not seen from **9a** to **8b** (Table 2). The small cone angle for **14c** (112.97°) compared with that for the PC_3 phosphorus in **8i** (123.44°) is somewhat curious. Not unexpectedly, the cone angle in **14a** (113.76°)[33] is close to that in **14c**[34] as are their respective CPC angles (97.37 and 96.06°).

(76) Akbayeva, D. N; Gonsalvi, L; Oberhauser, W; Peruzzini, M; Vizza, F; Brüggeller, P; Romerosa, A; Sava G; Bergamo, A. *Chem. Commun.* **2003**, 264−265.

(77) Chin, M.; Durst, G. L.; Head, S. R.; Bock, P. L.; Mosbo, J. A. *J. Organomet. Chem*, **1994**, *470*, 73−85.

The average NPN angle in **9a** [99.30(6)°, Table 1] is within 2.5° of that in $P(NMe_2)_3$ (102.1°).[43] The latter value is an average of the two $N_{ip}-P-N_{oop}$ angles (97.7°) and the $N_{oop}-P-N_{oop}$ angle (110.8°), where ip and oop denote the in-plane and out-of-plane angles relative to the mirror plane, respectively, present in this C_s symmetric molecule. The average O−P−O angle in bicyclic **3a** [102.07(13)°, Table 1] is virtually the same as that of the $P(OMe)_3$ conformer [102.1(9°)] present in the highest mole fraction (0.73, *anti*−*gauche*−*gauche* in the gas phase).[78] Thus, incorporating an acyclic PC_3, PN_3, or PO_3 acyclic framework into a bicyclo[2.2.2]octane structure such as **3a** or **9a** appears to result in only small changes in the corresponding C−P−C, N−P−N, or O−P−O angles. Formation of the bicyclic framework also does not seem to significantly alter the average P−O−C angle from that in $P(OMe)_3$ [118.79(10)°][78] to **3a** [122.15(17)°, Table 1] (whose values are within 2.6° of each other, when 3 × esd values are taken into account), nor the P−N−C angle in **9a** [118.79(10)°] from that in $P(NMe_2)_3$ [118.8°].[43] Because of the proximity of the nitrogen substituents R in the $P(NR)_3$ fragments (or lack of R in the case of **3a**), the cone angle at $PO_3/P(NR)_3$ in Table 2 varies from 106° (PO_3) to 155−169° [$P(NMe)_3$] to angles exceeding 180° (i.e., inverted cone angles) for $P(NPh)_3$.

Summary and Conclusions

The $^1J_{BP}$ data for the BH_3 adducts of $P(CH_2NMe)_3P$ (**8a**) are consistent with the PN_3 Lewis basicity order $MeC(CH_2NMe)_3P$ (**17a**) < $P(CH_2NMe)_3P$ (**8a**) < $(Me_2N)_3P$ < **15a** $N(CH_2CH_2NMe)_3P$. Furthermore, results of borane displacement experiments on $H_3BP(CH_2NMe)_3PBH_3$ (**8f**) with piperidine suggest that the B←PN_3 bond in **8f** is stronger than the B←PC_3 bond. Preferential PN_3 phosphorus coordination to BH_3 may be associated with back-bonding effects from the σ B−H BMOs into phosphorus orbitals, as has been invoked to account for the stability of F_3PBH_3.[79] Such effects would be expected to be much less for **8f** than for F_3PBH_3, although these influences would be facilitated by the unusually short N_3P-B distance in **8f** as discussed earlier.

The formation of *cis*-$Mo(CO)_4[P(CH_2NPh)_3P]_2$ (**9b**) and *cis*-$Mo(CO)_4[P(OCH_2)_3P]_2$ (**3w**) highlights the importance of steric versus electronic (presumably ligand π-acceptor) effects in the ligation of a $(PhN)_3P$ moiety versus a PO_3 fragment. The lower ν_{CO} IR frequencies of $W(CO)_5P(CH_2NMe)_3P$ (**8h**) than those for $W(CO)_5PMe_3$ suggest that the PC_3 phosphorus in **8a** is a better σ-donor/poorer π-acceptor than PMe_3, a conclusion supported by the shorter $W-PC_3$ distance in $W(CO)_5P(CH_2NMe)_3PW(CO)_5$ (**8i**) than in $(OC)_5W(PMe_3)$[63] and in **14c**.[34] A similar argument based on the shorter average $Mo-PC_3$ distance in *cis*-$Mo(CO)_4[P(CH_2NPh)_3PAuCl]_2$ (**9d**) compared with *cis*-$Mo(CO)_4(PMe_3)_2$ and the shorter average Ru−P distance in (η^5-C_5Me_5)-$Ru[P(CH_2NPh)_3P]_2$ (**9f**) compared with (η^5-C_5Me_5)$RuCl(PMe_3)_2$ leads to the same conclusion for ligand **9a**. In contrast, the higher ν_{CO} IR frequencies observed for *fac*-$Mo(CO)_3[P(CH_2NPh)_3P]_3$ (**9e**) compared with *fac*-$[Mo(CO)_3(PMe_3)_3]$ and *fac*-$[Mo(CO)_3$(**14a**$)_3]$ and the longer Mo−P and shorter *trans*-C≡O distances in **9e** compared with *fac*-$Mo(CO)_3$(**14a**$)_3$ are consistent with poorer σ-donor/better π-acceptor properties for **9a** than for PMe_3 or **14a**. The reason for this behavior in **9e** is not obvious. Perhaps mutual steric interactions among three phosphorus ligands in the *fac* configuration are particularly intense for **9a** with its paddle wheel arrangement of three phenyl groups, thus lengthening the Mo−P bond.

The X-ray-derived PC_3 cone angles for all the compounds in Table 2 except **8i** are within 3 × the esd of that for PMe_3. It is unclear why the PC_3 cone angle for **8i** is ca. 4° larger than the upper limit (119°) of the error range. Nonetheless, it is interesting that despite changes in polarizing power of the Z groups on the phosphorus in Table 2, the cone angles remain rather constant owing to constraint imposed by their bicyclic structures. Thus, the oxygen in $O{=}P(CH_2NMe)_3P$ (**8b**) opens the CPC angle by ca. 3° relative to **9a**, yet the cone angles for their $ZP(CH_2)_3$ moieties are within 2° of one another. However, from PMe_3 to $O{=}PMe_3$, the CPC angle opens ca. 7° and the cone angle increases about 8°.

The greater electronegativity of the PN_3 than the PC_3 phosphorus in **8a** is supported by the smaller value of $^1J_{PW}$ for the PC_3 (91.2 Hz) than that for the PN_3 (179.9 Hz) phosphorus in **8i**. The same relationship holds for $^1J_{PW}$ in $Me_3PW(CO)_5$ ($^1J_{PW}$ = 230 Hz)[64] compared with $(Me_2N)_3$-$PW(CO)_5$ ($^1J_{PW}$ = 314 Hz) and $MeC(CH_2NMe)_3PW(CO)_5$ ($^1J_{PW}$ = 321 Hz).[19c] This is consistent with the suggestion that the PN_3 phosphorus in these compounds has greater 1*s* density than the PC_3 phosphorus[80] owing to the more electronegative nitrogen.

Acknowledgment. We are grateful to the Petroleum Research Foundation administered by the American Chemical Society for a grant in support of this work.

Supporting Information Available: X-ray crystallographic files in CIF format for the structure determinations of compounds **3a**, **8b**,**f**,**i**, and **9a**,**d**,**e**,**f**. This material is available free of charge via the Internet at http://pubs.acs.org.

IC0703070

(78) Belyakov, A.; Dalhus, B.; Haaland, A.; Shorokhov, D. J.; Volden, H. V. *J. Chem. Soc., Dalton Trans.* **2002**, 3756−3762.
(79) Beach, D. B.; Jolly, W. L. *Inorg. Chem.* **2002**, *24*, 567−70.
(80) (a) Cowley, A. H.; Mills, J. H.; *J. Am. Chem. Soc.* **1969**, *91*, 2915−2919. (b) Keiter, R. L.; Verkade, J. G. *Inorg. Chem.* **1969**, *8*, 2115−2120.